FULL REPORT

Crosslinked Silk Fibroin Hydrogel for Controlled Release of Natural α-Mangostin

By

Dr. Patchara Punyamoonwongsa
Dr. Suwanna Daechathai

This research was supported by
National Research Council of Thailand
Research Fund Budget Year 2013

ACKNOWLEDGEMENT

There are a number of people whose help with this project has been invaluable. The first are my lovely students, Nuchada Suttenun and Ngampuk Tayana, who had been working hard side-by-side with me in the laboratory. I would like to thank the Silk Innovation Center, Mahasarakham University, for providing me with the Thai *Bombyx mori* silkworm cocoons. Thanks are also due to all staffs in the Scientific and Technological Instruments Center, at Mah Fah Luang University, for their constantly helps and generous access to equipment. I would also like to thank my dear parents, sister and brother for their understanding and unconditional love. Last but not least, I wish to express my appreciation to the National Research Council of Thailand (NRCT) and Mae Fah Luang University for their financial support throughout this research project.

Dr. Patchara Punyamoonwongsa

Dr. Suwanna Deachathai

November 2014

EXECUTIVE SUMMARY

Naturally-derived hydrogels from the *Bombyx mori* silk fibroin (SF) have recently been attracted interest from many researchers as promising biomaterials due to their biocompatibility, ease of fabrication, water absorbability and non-cytotoxicity. Despite these, natural silk gelation is normally too long and uncontrollable. Moreover, unmodified SF hydrogels are rather brittle and not stable in an aqueous media thus, limiting their practical uses in both tissue engineering and biomedical fields. To overcome these drawbacks, the new physical and chemical crosslinking methods were proposed to stabilize SF hydrogels through the formation of stable interconnected network structure. The physically and chemically crosslinked hydrogels were prepared under physiological conditions by incubation of aqueous SF solutions with poly(ethylene glycol)diacrylate (PEGDA) and, *O'O*-bis[2-(*N*-succinimidyl succinylamino)ethyl]polyethylene glycol (NHSP), respectively. Various parameters were optimized on the basis of hydrogel properties, including the gelation time, water resistance and interior morphology. Different analytical techniques, such as Sodium Dodecyl Sulfate Polyacrylamide Gels Electrophoresis (SDS-PAGE), Fourier Transform Infrared (FTIR) spectroscopy, Scanning Electron Microscopy (SEM), Differential Scanning Calorimetry (DSC), Thermogravimetric Analysis (TGA) and antimicrobial assay, were employed to evaluate the crosslinking efficiency of all-aqueous approaches to tailor the SF-based materials for a sustained therapeutic delivery of a natural extract α-mangostin. This study was expected, not only to provide valuable details for appropriate SF hydrogel design in tissue engineering and biomedical fields, but also to add values to both agricultural and sericulture products in Thailand.

ABSTRACT

Hydrogels from the *Bombyx mori* silk fibroin (SF) are of great interest for drug delivery and tissue engineering applications because of their biocompatibility, water absorbability, controllable biodegradation rate and processability into different formats. Despite these, unmodified SF samples normally display poor mechanical strength with prolonged gelation kinetics thus, limiting their practical use in biomedical applications. To overcome these drawbacks, the new all-aqueous crosslinking methods to form the three-dimensional (3D) porous SF hydrogel network were developed. The physically crosslinked SF hydrogels were prepared by mixing different aqueous SF solutions (2-10% w/v) with poly(ethylene glycol)diacrylate (PEGDA). All formulations were then, incubated at room temperature until there is a pronounced increase in the apparent viscosity. Results indicated that PEGDA (30% w/v) could successfully shorten the silk gelation time and stabilize the silk hydrogels in aqueous media. This was associated with a formation of the interconnected sheet-like structure, as observed by Scanning Electron Microscopy (SEM). Data interpretation of Fourier Transform Infrared (FTIR) spectra suggested that the PEGDA-induced gelation was driven by a conformational transition of SF from α-helix into the β-sheet structure. Furthermore, the process was affected by the type of extraction solvent and the utilization of sonication. Surprisingly, the physically crosslinked hydrogels exhibited moderate antibacterial activity against gram positive *Bacillus cereus*, MRSA-SK1 and *Staphylococcus aureus*, as evidenced by the diameters of the inhibition zone between 9.2-10.9, 5.7-6.1 and 5.7-6.2 mm, respectively. This finding highlighted another unexploited property of the hybrid in biomedical fields.

Apart from a physical method, a new chemical modification by using a protein crosslinker, *O'O*-bis[2-(*N*-succinimidyl succinylamino)ethyl]polyethylene glycol (NHSP), was also employed to fabricate the more stable SF hydrogels. For this, appropriate amounts of NHSP was mixed with an aqueous SF solution at room temperature in the presence of poly(*L*-lysine) (PLL) as a gel enhancer. A network formation was accelerated by the using of ultrasonication and noticed within 24 hours, depending on the silk concentration. A crosslink reaction was convinced by the

appearance of a new ether linkage observed in the Fourier-transform Infrared (FTIR) spectra, and the presence of a new thermal decomposition temperature (T_d) in the Thermogravimetric Analysis (TGA) thermograms. Such crosslinking contributed to the improved hydrogel properties, such as a structural integrity, thermal stability and water-resistance. Also, this produced an interconnected porous structure with higher β-pleated sheet content, comparing to the physically crosslinked ones. These two new methods thus, proven to be capable of improving both gelation kinetics and physicochemical properties of SF, making it more suitable for both biomedical and tissue engineering applications.

บทคัดย่อ

ไฮโดรเจลจากไหมบอมบิกซ์ มอริ ไฟโบรอิน (SF) กำลังได้รับความสนใจในการนำมาใช้งานด้านการขนส่งตัวยา และวิศวกรรมเนื้อเยื่อ ทั้งนี้ เนื่องมาจากความเข้ากันได้ทางชีวภาพกับเซลล์ การดูดซึมน้ำ อัตราการย่อยสลายทางชีวภาพที่ควบคุมได้ และการขึ้นรูปได้อย่างหลากหลาย นอกเหนือไปจากข้อดีดังกล่าว ตัวอย่างไฟโบรอินที่ไม่ได้ถูกดัดแปลง มักจะมีค่าความแข็งแรงเชิงกลต่ำ อีกทั้ง ยังมีจลนศาสตร์การเกิดเจลที่ค่อนข้างจะยาวนาน ทำให้การประยุกต์ใช้งานทางการแพทย์ของวัสดุไฟโบรอินมีขอบเขตจำกัด งานวิจัยนี้ ได้พัฒนาวิธีการแบบใหม่ สำหรับใช้เตรียมไฮโดรเจลไฟโบรอินที่มีโครงสร้างแบบเชื่อมขวาง และมีรูพรุนถักทอกันเป็นแบบสามมิติ วิธีการแรก เป็นการใช้เตรียมไฮโดรเจลไฟโบรอินที่มีการเชื่อมขวางทางกายภาพ โดยการผสมสารละลายไฟโบรอิน (ร้อยละ 2-10 โดยมวลต่อปริมาตร) เข้ากับ พอลิ(เอทิลีน ไกลคอล) ไดอะคริเลต (PEGDA) แล้วทำการบ่ม ณ อุณหภูมิห้อง จนกว่าสารละลายจะมีความหนืดที่สูงขึ้นที่สามารถต้านทานการไหลของของเหลวได้ ผลการทดลองพบว่า การเติม PEGDA (ร้อยละ 30 โดยมวลต่อปริมาตร) ช่วยลดระยะเวลาในการเกิดเจล และช่วยเพิ่มเสถียรภาพของไฮโดรเจลไฟโบรอินในตัวกลางที่เป็นน้ำ ทั้งนี้ อาจเนื่องมาจากการเกิดโครงสร้างแบบแผ่นทับซ้อนที่มีการเชื่อมโยงอย่างทั่วถึงกันของโฟโบรอิน ซึ่งสามารถพิสูจน์ให้เห็นได้จากเทคนิคกล้องจุลทรรศน์อิเลคตรอนแบบส่องกราด การวิเคราะห์ผลจากเทคนิคอินฟราเรดสเปคโตรสโคปี ยังแสดงให้เห็นอีกว่า การเปลี่ยนโครงรูปของไฟโบรอินจากแบบเกลียวไปเป็นแบบแผ่นทับซ้อน เป็นแรงผลักดันที่สำคัญต่อกระบวนการเร่งให้เกิดเจลโดย PEGDA นอกจากนี้แล้ว ชนิดของสารละลายที่ใช้ในกระบวนการสกัดไฟโบรอิน ตลอดจนการกระตุ้นโดยการใช้คลื่นอุลตราโซนิกส์ ล้วนแล้วแต่มีผลต่อจลนศาสตร์การเกิดเจลของไฟโบรอิน สิ่งที่น่าสนใจอีกประการหนึ่งของไฮโดรเจลไฟโบรอินที่มีโครงสร้างแบบเชื่อมขวางทางกายภาพ คือ ความสามารถในการยับยั้งการเจริญเติบโตของเชื้อแบคทีเรียที่ทำให้ก่อโรค 3 ชนิด คือ *Bacillus cereus*, MRSA-SK1 and *Staphylococcus aureus*

โดยทำให้เกิดบริเวณของการยับยั้งในช่วง 9.2-10.9, 5.7-6.1 และ 5.7-6.2 ม.ม. ตามลำดับ คุณสมบัติที่ค้นพบใหม่นี้ ทำให้วัสดุผสมไฟโบรอินมีความเป็นไปได้ และมีความเหมาะสมเป็นอย่างยิ่งต่อการใช้งานทางการแพทย์

นอกเหนือไปจากการเชื่อมขวางทางกายภาพแล้ว การศึกษานี้ ยังได้พัฒนาอีกหนึ่งวิธีการ สำหรับใช้เตรียมไฮโดรเจลไฟโบรอินที่มีการเชื่อมขวางโดยพันธะเคมี ที่มีทั้งความแข็งแรงและเสถียรภาพที่สูงมากขึ้น ในการนี้ ได้ทำการผสมสารละลายไฟโบรอินเข้ากับสารเชื่อมขวาง *O'O*-Bis[2-(*N*-succinimidyl succinylamino)ethyl]polyethylene glycol (NHSP) และพอลิแอลไลซีน (PLL) ณ อุณหภูมิห้อง จากการศึกษาพบว่า คลื่นอุลตราโซนิกซ์สามารถเร่งให้เกิดโครงสร้างแบบเชื่อมขวางได้ภายในระยะเวลา 24 ช.ม. ซึ่งก็ขึ้นอยู่กับความเข้มข้นของสารละลายไฟโบรอินที่ใช้ด้วยเช่นกัน การเชื่อมขวางของไฟโบรอินโดย NHSP ถูกพิสูจน์ได้จากการตรวจพบการดูดกลืนรังสีอินฟราเรดของหมู่ฟังก์ชันใหม่ คือ อีเทอร์ และการพบสัญญาณการสลายตัวทางความร้อนใหม่ ณ อุณหภูมิที่สูงขึ้น โครงสร้างแบบเชื่อมขวางโดยพันธะเคมีที่เกิดนี้ทำให้ไฮโดรเจลไฟโบรอินมีเสถียรภาพทางโครงสร้าง ทางความร้อน และการละลายน้ำที่ดีขึ้น นอกจากนี้แล้ววิธีการเชื่อมขวางดังกล่าว ยังสามารถทำให้เกิดรูพรุนสามมิติที่ต่อเนื่อง ที่มีปริมาณแผ่นซ้อนทับของไฟโบรอินที่มากกว่าวิธีการเชื่อมขวางแบบกายภาพอีกด้วย การศึกษาครั้งนี้ จึงแสดงให้เห็นถึงประสิทธิภาพของวิธีการเชื่อมขวางทั้งสอง ที่สามารถนำมาใช้เพื่อเร่งจลนศาสตร์การเกิดเจลของโปรตีนไฟโบรอิน และเพื่อปรับปรุงคุณสมบัติทางกายภาพเคมีของไฮโดรเจลไฟโบรอินให้มีความเหมาะสมต่อการประยุกต์ใช้งานด้านการแพทย์และวิศวกรรมเนื้อเยื่อ

LIST OF CONTENTS

LIST OF TABLES

LIST OF FIGURES

LIST OF ABBREVIATIONS AND SYMBOLS

SF	=	Silk fibroin
RSF	=	Regenerated silk fibroin
NHS	=	*N*-Hydroxysuccinimide
EGS	=	Ethylene glycolyl bis(succinimidyl succinate)
NHSP	=	*O'O*-Bis[2-(*N*-succinimidylsuccinylamino) ethyl]polyethylene glycol
PLL	=	Poly-*L*-lysine
PEGDA	=	Poly(ethylene glycol)diacrylate
MeOH	=	Methanol
EtOH	=	Ethanol
Me_2CO	=	Acetone
Acetone-d_6	=	Deuterated acetone
TMS	=	Tetramethylsilane
DMSO	=	Dimethyl sulfoxide
NSS	=	Normal saline solution
B. cereus	=	*Bacillus cereus*
E. coli	=	*Escherichia coli*
MRSA	=	Methicillin resistant *Staphylococcus aureus*
Ps. aeruginosa	=	*Pseudomonas aurenginosa*
S. typhimurium	=	*Salmonellae typhimurium*
S. aureus	=	*Staphylococcus aureus*
MICs	=	Minimum inhibition concentrations
IC_{50}	=	50% inhibition concentration
MHB	=	Mueller hinton broth
CFU	=	Colony forming unit
FTIR	=	Fourier transform infrared
UV-Vis	=	Ultraviolet-visible
^{1}H-NMR	=	Proton nuclear magnetic resonance
2D-NMR	=	Two dimensional nuclear magnetic resonance
^{13}C-NMR	=	Carbon nuclear magnetic resonance
TLC	=	Thin-layer chromatography

LIST OF ABBREVIATIONS AND SYMBOLS

DSC	=	Differential scanning calorimetry
TGA	=	Thermogravimetric analysis
SEM	=	Scanning electron microscopy
QCC	=	Quick column chromatography
CC	=	Column chromatography
%	=	Percentage
% v/v	=	Percentage of volume by volume
% w/v	=	Percentage of weight by volume
% w/w	=	Percentage of weight by weight
μM	=	Micromolar
ppm	=	Part per million
^{o}C	=	Degree celsius
min	=	Minute
hr	=	Hour
cm^{-1}	=	Wavenumber
T_d	=	Degradation temperature
T_m	=	Crystalline melting temperature
m.p.	=	Melting point
kg	=	Kilogram
g	=	Gram
mg	=	Milligram
μg	=	Microgram
mL	=	Milliliter
mm	=	Millimeter
cm	=	Centimeter
nm	=	Nanometer
δ	=	Chemical shift relative to TMS
J	=	Coupling constant
s	=	*Singlet*
d	=	*Doublet*
t	=	*Triplet*

LIST OF ABBREVIATIONS AND SYMBOLS

HMBC	=	Heteronuclear multiple bond correlation
Hz	=	Hertz
MHz	=	Megahertz
λ_{max}	=	Maximum wavelength
γ_{max}	=	Major bands
ε	=	Molar extinction coefficient
rpm	=	Revolutions per minute
S.D.	=	Standard deviation

CHAPTER 1
INTRODUCTION

1.1 Research Problem

Hydrogels are hydrophilic three-dimensional networks of polymeric chains capable of absorbing up to thousands of times their dry weight in water (Teng et al., 2010, Farris et al., 2009). Their ability to mimic body tissues and respond to external stimuli offers them promising materials for various biomedical applications including tissue engineering, drug controlled release systems and biosensors (Teng et al., 2010, Kweon et al., 2001, Farris et al., 2009, Mandal et al., 2009b). To encapsulate and delivery cells or other therapeutic compounds, hydrogels must be formed without damaging the bioactive molecules, biocompatible, suitable mechanical properties and controllable biodegradability. A variety of synthetic and naturally derived materials have been used to form hydrogels. The benefits of synthetic polymers include their controllable gelation and great reproducibility of hydrogel characteristics (Wang et al., 2008). However, most of them are relatively hydrophobic and in some cases, further chemical modifications are needed to make it more suitable and biocompatible for the practical uses (Gomes et al., 2012).

Natural polymers such as fibrin, collagen, silk, chitosan, alginate and hyaluronic acid are widely used in tissue engineering (Gomes et al., 2012, Garcia-Fuentes et al., 2008, Mandal et al., 2009a, Zhang et al., 2011b). Among all available sources, polypeptides have received much attention as a new class of material due to their intrinsic biocompatibility, biodegradability, mechanical durability, and natural abundance. They also allow chemically functionalization with bioactive molecules as well as support cells attachment and proliferation (Gomes et al., 2012). Natural silk-fibroin (SF) derived from the *Bombyx mori* silk cocoons, is one of the most outstanding fibrous proteins recently, been used as biomaterials. Its superior properties include excellent mechanical properties, biocompatibility, controllable biodegradation rate, processability into different formats and inducible formation of the crystalline β-pleated sheet structure (Gomes et al., 2012, Wang et al., 2008, Rouse and Kyke, 2010, Acharya et al., 2008) The ability of SF to self-assemble into the gel-like structures, in response to stimuli factors highlights it a promising material for cell

encapsulation, nerve generation, wound dressing and tissue engineering scaffolding. SF gel can be prepared by many methods including dehydration, incubation at high concentration and ionic strength, heating, acidification and sonication (Wang et al., 2008, Jin et al., 2005, Chen et al., 2008b). For biomedical application, gelation must be induced under mild conditions in a short period of time. However, silk gelation time is usually long unless non-physiological treatments are considered (Wang et al., 2008, Jin et al., 2005). Moreover untreated SF samples are rather brittle that does not provide sufficient mechanical strengths. They are also not stable in an aqueous media, thus to some extent limiting their use in biomedical fields. Thus, there is a need to develop more efficient ways to shorten the silk gelation time while managing its biodegradability over a period of time.

Chemical modification by using crosslinking reagents is another promising approach to fabricate the biopolymer gel with improved mechanical strength, flexibility and water solubility. Many crosslinking reagents were chosen to form crosslinked SF networks, such as glutaraldehyde, formaldehyde, carbodiimides hydrochloride (EDC), *N,N'*-methylenebis acrylamide and tyrosinase (Kang et al., 2004, Bayraktar et al., 2005, Kweon et al., 2001, Mandal et al., 2009b). Nevertheless, some of the crosslinking reagents provoked cytotoxicity or immunogenicity and the crosslinking reaction may essentially require specific binding sites under specific or harsh conditions. Therefore, an alternative non-toxic crosslinking agent that efficiently produces stable and biocompatible SF hydrogels with enhanced mechanical properties is needed to overcome these drawbacks.

A new sort of crosslinking agent, *O'O*-bis[2-(*N*-succinimidyl succinylamino)ethyl]polyethylene glycol or NHSP (chemical structure shown in Figure 1.1), is of interest mainly due to its cytocompatibility and biocompatibility. NHSP is synthesized by the reaction between a carboxylic acid and *N*-hydroxysuccinimide (NHS) in the presence of carbodiimides (Zhang et al., 2011a, Abdella et al., 1979). NHSP is a bifunctional reagent for the crosslinking and reversible immobilization of proteins through the amine-reactive NHS esters at both ends of the spacer arm. It reacts rapidly with proteins at pH 8-9 and at high dilution. Trypsin, immobilized on agarose using this reagent, retained full specific activity, stable and could be released with hydroxylamine at 25°C (Abdella et al., 1979).

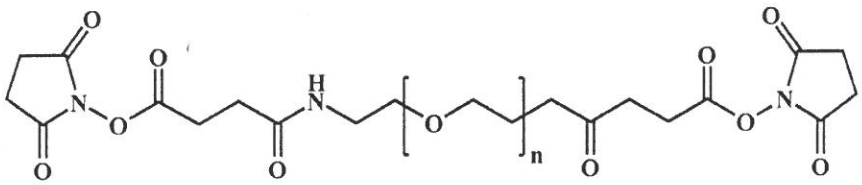

Figure 1.1 Chemical structure of NHSP crosslinking agent used in this study.

This project proposed a novel method to chemically crosslinking the *B. mori* SF protein by using the non-toxic homobifunctional NHSP crosslinking agent under physiological conditions. To enhance the crosslinking reactions, appropriate amount of poly-*L*-lysine (PLL) was mixed together with SF in the presence of the crosslinker. The crosslinked network was expected to be formed through acylation reaction between the free amino pendant groups of the proteins and the active NHSP at both ends (Abdella et al., 1979). Various physicochemical and biological properties, as well as the structural integrity of the resultant gels, *including* morphology, water swelling ability and thermal properties, were evaluated by using different techniques such as Sodium dodecyl sulfate-Polyacrylamide gel electrophoresis (SDS-PAGE), Differential scanning calorimetry (DSC), Thermogravimetric analysis (TGA), Fourier transform infrared (FTIR) spectroscopy, Scanning electron microscopy (SEM) and antimicrobial assay.

Beside a chemical crosslinking, a new all-aqueous physical crosslinking method was also employed to speed up the silk gelation process and to enhance the material properties. The poly(ethylene glycol)diacrylate (PEGDA) was chosen as an inducer to alter the hydration sphere around SF molecules and then, allow them to self-aggregate into a crystalline β-pleated structure. This inducer (chemical structure shown in Figure 1.2) is a synthetic, biodegradable and biocompatible polymer with very low toxicity and excellent solubility in aqueous solutions (Tan and Marra, 2010, Qiu et al., 2003). Furthermore, the material has been widely used for many applications. For example, as the cell scaffolds, biomedical adhesive and delivery vehicles (Qiu et al., 2003). The effects of several relevant factors, including the types of extraction solvent (e.g., LiBr, or a ternary CaCl2/EtOH/Water) and a combined using of ultrasonication and the PEGDA addition, were also evaluated in this study. Furthermore, the crosslinking efficiency of both the physical and chemical methods was also examined on the basis of different

hydrogel properties using both physical and analytical techniques. The release kinetics of different crosslinked hydrogels will also be investigated in the near future, using a model compound such as a natural extract, α-mangostin, for their potential uses in both tissue engineering and controlled drug release applications. Biological activities of α-mangostin, derived from the fruit peels of the economic crop of Thailand, *Garcinia mangostana* Linn., have been earlier reported. Xanthone compounds, such as α-, β- and γ-mangostins, mangostenol and mangostenone, were recognized as major compounds of the natural extract *G. mangostana* (Pedraza-Chaverri, 2008). These compounds, particularly α-mangostin, exhibit anti-oxidant, anti-tumor, anti-inflammatory, anti-allergy and antibacterial activities (Pedraza-Chaverri, 2008, Matsumoto et al., 2004, Jung et al., 2006, Nakagawa et al., 2007, Gopalakrishnan et al., 1980, Chairungsrilerd et al., 1996, Chen et al., 2008a, Yoshikawa et al., 1994, Williams et al., 1995, Mahabusarakam et al., 2000, Sundaram et al., 1983).

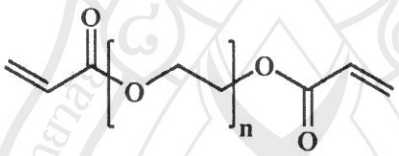

Figure 1.2 Chemical structure of PEGDA.

The current research project was expected not only, to develop new silk-based biomaterials, but also to add values to both agricultural and sericulture products. We also hoped that this project would provide valuable details to lay groundwork for silk and natural product technologies.

1.2 Objectives

1.2.1 To prepare the crosslinked silk-fibroin (SF) hydrogels using nontoxic *O'O*-bis[2-(*N*-succinimidyl succinylamino)ethyl]polyethylene glycol (NHSP) and poly(ethylene glycol)diacrylate (PEGDA) as a crosslinking agent and inducer, respectively.

1.2.2 To evaluate the efficiency of the new crosslinking methods on the basis of;

- Gelation time
- Structural aspect
- Water resistance (e.g., sol-gel fraction)

- Rheological properties
- Thermal stability
- Morphological details
- Controlled release character
- Cell cytotoxicity

1.2.3 To evaluate the biological activity of a natural extract α-mangostin released from the silk fibroin hydrogels.

1.3 Scope of Research

The study was split into 6 parts as described below.

Part 1: This part included fundamental characterization of regenerated SF and the studying of *in vitro* SF gelation. Various physicochemical properties of SF and some factors affecting its gelation process were determined as a mean to gain better understanding of a silk gelation process for the subsequent crosslinking reactions. Different physicochemical properties are listed below.

- Gelation time
- Sonication
- Rheological properties
- Molecular weight range and protein purity
- Structural, conformational and morphological details
- Thermal properties
- Water swelling ability (water-resistance or sol-gel fraction)

Part 2: This was performed in parallel to PART 1 and accounted for the extraction and structural analysis of α-mangostin isolated from fruit peels of *G. mangostana*, using chromatographic and spectroscopic techniques.

Part 3: This was a preparation of crosslinked SF hydrogels using NHSP and PEGDA as a crosslinking agent and inducer, respectively. The following are important parameters needed to be evaluated.

- A mass ratio of SF to the crosslinking agent (or inducer)
- The effect of PLL addition on the chemical crosslinking of SF and NHSP
- Utilization of sonication

Part 4: This part was a further characterization of the SF hydrogels obtained from Part 3 by using different analytical techniques. Various physicochemical properties of the hydrogels are listed below.

- Gelation time
- Rheological properties
- Molecular weight range and protein purity
- Structural and conformational details
- Morphological details
- Thermal properties
- Water swelling ability (water-resistance or sol-gel fraction)
- Drug encapsulation and controlled release
- Cytotoxicity

Part 5: This part aimed to evaluate antibacterial activity of α-mangostin both before and after encapsulation into SF hydrogels.

Part 6: This was a wrap-up session to systematically evaluate potential use of the novel crosslinking methods for a preparation of the crosslinked SF hydrogels as a drug delivery matrix with improved physicochemical properties.

CHAPTER 2
LITERATURE REVIEW

2.1 Hydrogels

Hydrogels have received much attention from scientists for many years. They are three-dimensional (3D) polymeric networks and resistant to swell in an aqueous solution without losing its structural integrity. They have impressively high degree of water content thus, mimicking some tissues and extracellular matrices (ECM) (Sah and Pramanik, 2011). Hydrogels are suitable for biomedical applications, for example as the controlled drug release devices, biosensors, contact lenses, immobilization carriers, cell culture matrices as well matrices to repair and regenerate a wide range of tissues and organs in tissue engineering technology (Hoffman, 2002, Mandal et al., 2009b). For these, hydrogels must be prepared without destroying the encapsulated compound while, maintaining its biocompatibility, and other superior properties. One of many advantages of hydrogel is a great variety of methods to establish the crosslinking within the polymer matrices. Generally, the hydrogel network can be formed by either a chemical or physical method (Wang et al., 2008). The physical crosslinking hydrogels are formed by the molecular entanglements or secondary forces of polymer such as the ionic attraction, hydrogen bonding and hydrophobic interactions. The chemical crosslinking hydrogels are obtained by forming a covalent bond between the polymer chains through redox, photo or thermal polymerization reaction. Physically crosslinked gels are of interest for both biomedical and pharmaceutical applications because the gels formed are more compatible for hosting cells (Hoffman, 2002, Ko et al., 2013). Despite this benefit, the physical crosslinking reactions are less controllable and the morphology of the resultant gels is varied. Chemically crosslinked hydrogels are more reproducible, tunable and display excellent properties (Hennink and Nostrum, 2002, Wang et al., 2008). However, due to a non-physiological method used, the encapsulated compound such as proteins, drugs and cells may be damaged during a hydrogel network formation. Beside this fact, the sources of the material also influence biological properties of hydrogels. For example, hydrogels from synthetic polymers display less biocompatibility thus, limiting their use as biomaterials (Wang et al., 2008, Hardy et

al., 2008). Hydrogels from biopolymers, such as polysaccharides and poly(amino acids), are more compatible and their degradation products produced are non-toxic. This means that the compounds formed can either be metabolized into harmless products or excreted by the renal filtration process (Hennink and Nostrum, 2002).

2.2 Silk Fibroin

Silk fiber is a protein-based material made by arthropods for a variety of task-specific applications (Hardy et al., 2008). It has recently attracted interest from all researchers as an ideal material for a wide range of applications, especially in biomedical and tissue engineering fields as controlled delivery matrices. Silk solution can be morphed into different formats including films, 3D porous scaffolds, hydrogels, micro- and nanospheres, nanofibers and coating (Numata and Kaplan, 2010). Silk proteins are biocompatible and biodegradable with good mechanical properties and water absorption (Wang et al., 2008). The degradation rate of the silk biomaterials can be controlled during processing by altering the extent of secondary structure in the silk protein (Numata and Kaplan, 2010). *Bombyx mori* silk fiber composes of two types of proteins, sericin and fibroin. Sericin, the antigenic gum-like protein is located on the fiber surface. Fibroin fibrils, the main structural component of the fiber, are located at the core of the fiber and glued together by sericin. Filaments of fibroin comprise of highly organized β-sheet crystal and semicrystalline regions (Altman et al., 2003) (Figure 2.1). Sericin acts as an adhesive to maintain the fiber and the multi-layer structure in the whole cocoon (Chen et al., 2012).

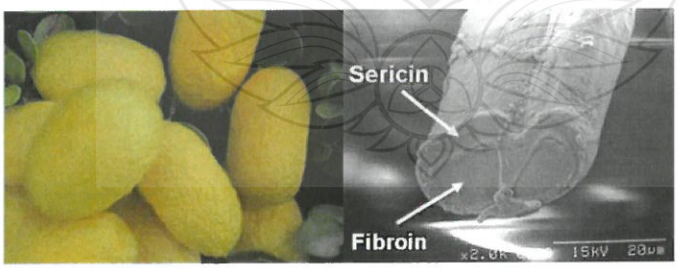

Figure 2.1 *B. mori* silk cocoons (left) and cross-section of the silk fiber (right). (Pictures modified from http://www.hiroshima-u.ac.jp)

B. mori silk fibroin is a fibrillar protein (Nagarkar et al., 2010) that consists of two major components, light (~25 kDa) and heavy chains (~325 kDa), bonded together by single disulfide bond (Matsumoto et al., 2006, Numata and Kaplan, 2010). The chemical composition of silk fibroin consists of residues of no less than 16 amino acids whose ratio varies between different areas of the supramolecular structure (Table 2.1) (Sashina et al., 2006). The primary structure of fibroin composes of predominance (ca. 90%) amino acids, glycine, alanine, serine, valine and tyrosine, with characteristic repetitive sequences of GAGAGS, GAGAGY and GAGAGVGY (Matsumoto et al., 2006). The highly repetitive sections are composed of glycine, alanine and serine as $[gly\text{-}ala\text{-}gly\text{-}ala\text{-}gly\text{-}ser]_n$. These three amino acids contain short side chains that permit close packing through the stacking of hydrogen-bonded β-sheets (Chen et al., 2001). The high content of hydrophobic glycine-alanine repeats (Heavy chain) gives rise to the crystalline nature of silk fibers (Li et al., 2002). The Light chain is more hydrophilic and relatively elastic (Hardy et al., 2008).

Table 2.1 Amino acid composition of *B. mori* fibroin (Sashina et al., 2006).

Amino acid	Composition (% mol)		
	Total	Heavy areas	Light areas
Glycine	42.9	49.4	10.0
Alanine	30.0	29.8	16.9
Serine	12.2	11.3	7.9
Tyrosine	4.8	4.6	3.4
Valine	2.5	2.0	7.4
Aspartic acid	1.9	0.65	15.4
Glutamic acid	1.4	0.70	8.4
Threonine	0.92	0.45	2.8
Phenylalanine	0.67	0.39	2.7
Methionine	0.37	-	0.37
Isoleucine	0.64	0.14	7.3
Leucine	0.55	0.09	7.2
Proline	0.45	0.31	3.0
Arginine	0.51	0.18	3.8
Histidine	0.19	0.09	1.6
Lysine	0.38	0.06	1.5

B. mori silk fibroin has two different structural conformations, termed silk I (random coil) and silk II (β-sheet) (Chen et al., 2001). A hydrophobic secondary structure of SF is an antiparallel β-sheet which are composed of relatively large hydrophilic chain end blocks (N- and C- terminal) with smaller hydrophilic internal blocks and large internal hydrophobic block (Matsumoto et al., 2006). The structure of silk fibroin consists of the coexisting amorphous and crystalline domains of which the peptide chains are bounded together by hydrogen bonds to form sheet like crystalline structures (Nagarkar et al., 2010). The natural silk gelation process occurs because silk fibroin chains tend to aggregate, transforming from an amorphous conformation (random coil) to a more stable structure (β-sheet) (Nogueira et al., 2011). The conformational transition of silk fibroin structure has been studies by using different methods and it is commonly known as a "sol-gel transition" or a "protein aggregation". The silk fibroin forms colloidal aggregates, driven by the van der Waals forces, electrostatic interactions, hydrogen bonding and hydrophobic interactions (Chen et al., 2001, Mondal et al., 2007).

2.3 Accelerated Silk Gelation

Although, silk fibroin hydrogels exhibits impressive physicochemical and biological properties, however, the practical uses of these silk-based materials in biomedical and tissue engineering applications are still limited due to their poor water-resistance and relatively long gelation time (Matsumoto et al., 2006). Practically, gelation must be induced under mild conditions within a relatively short period of time (2-3 hours) to avoid cell damage (Wang et al., 2008). Many factors, such as temperature, pH, ionic strength and silk fibroin concentration, have been reported to affect the gelation kinetics in the regenerated silk fibroin solution. All these play important role on a structural transition from a random coil (α-helix) to a β-sheet and thus, a hydrogel network formation (Wang et al., 2008, Numata and Kaplan, 2010, Xiong et al., 2011). A mechanism of silk gelation and its influencing factors has been studies by many researchers as a mean to accelerate the silk gelation time. For example, methanol was used to induce a conformational transformation of silk fibroin from a random coil to a β-sheet structure. The method introduces more physical crosslinking sites for the hydrogel network formation and renders it a water-insoluble

with slower-biodegradability (Xiong et al., 2011, Motta et al., 2004). Alternatively, a water annealing method was also developed to induce such transition without the use of any organic solvent (Wang et al., 2008, Numata and Kaplan, 2010).

Additionally, gelation of silk fibroin could be induced by the increasing of silk fibroin concentration and incubation at high temperatures. Relationships between gelation time and the silk fibroin concentration at different incubation temperatures are shown in Figure 2.2. The result indicated that gelation time decreases with the increased fibroin concentration and temperature (Matsumoto et al., 2006). The sol-gel transition of fibroin arises from a combination of inter- and intramolecular interactions including hydrophobic interactions and hydrogen bonds which leads to a β-sheet formation and so a physical crosslinking. The accelerated gelation at higher temperature can be explained by the dynamics of hydrophobic hydration around the polypeptide.

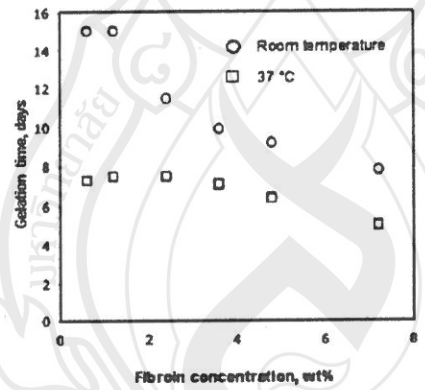

Figure 2.2 Concentration-dependent fibroin gelation time at (○) room temperature and (□) 37 °C determined from optical density changes at 550 nm (Matsumoto et al., 2006).

Effect of pH on the silk fibroin gelation was previously examined and is shown in Figure 2.3. The result indicated that gelation time increases with the increased pH solution. Furthermore, a shorter gelation time was observed for the higher fibroin concentration. The acidification is important for the silk fibroin gelation rate. This is because the acidic pH reduces hydrophilicity and charge repulsion that promote hydrophobic interactions, physical crosslinking and kinetic gelation of fibroin molecules (Matsumoto et al., 2006).

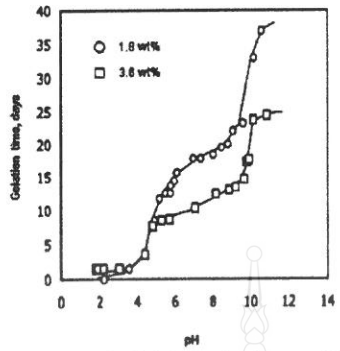

Figure 2.3 Relationships between initial solution pH and gelation time at room temperature determined by change in the optical density for (○) 1.8 and (□) 3.6 wt% (Matsumoto et al., 2006).

Recent studies by Wang and co-workers illustrated that the using of sonication could speed up the silk gelation. It was found that silk gelation time decreases with the increased sonication time (Figure 2.4). During sonication, the mechanical vibration causes the formation and collapse of bubbles that generates extremely large energies on localized scale for short periods of time. This process accelerates the formation of physical crosslinking, such as initial chain interactions related to a β-sheet formation (gel), due to changes in hydrophobic hydration (Wang et al., 2008).

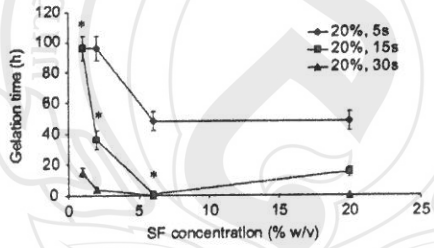

Figure 2.4 Silk fibroin gelation time under various sonication conditions; 5 (●), 15 (■) and 30 (▲) seconds (Wang et al., 2008).

Although, the methods proposed earlier could accelerate the silk fibroin gelation, however, most of the methods used required non-physiological treatments which could be harmful for the encapsulated active compounds such as drugs or cells. Therefore, there is a need to develop a method to accelerate the silk gelation while maintaining its biocompatibility, biodegradability, promoting cell migration and antiogenesis, together with allowing rapid nutrient diffusion (Dhandayuthapani et al., 2011).

2.4 A Novel Protein Crosslinking

Our pilot study revealed that the addition of poly(ethylene glycol) diacrylate (PEGDA), chemical structure shown in Figure 1.2, could speed up the gelation kinetics of SF. It was thus, worth performing additional experiments to systematically clarify this effect. PEGDA is a synthetic polymer, water-soluble, non-toxic, biodegradable and biocompatible material (Qiu et al., 2003, Tan and Marra, 2010). It has been widely used for many applications including as cell scaffolds, biomedical adhesive and delivery vehicles. This solvent-free method would allow a formation of physically crosslinked fibroin network at physiological pH and temperature, making the material more suitable as injectable scaffolds and *in situ* drug delivery matrices (Crompton et al., 2007), while maintain its superior biocompatibility and biodegradability.

Apart from these, the chemically crosslinked hydrogels are still one of the best candidate for a wide range of biomedical applications (Tan and Marra, 2010) due to their controllable crosslinking density and structural properties. In this project, the new covalently crosslinked SF hydrogels are prepared by using a *O'O*-bis[2-(*N*-succinimidyl succinylamino)ethyl]polyethylene glycol (NHSP) as a crosslinking agent. NHSP is a homobifunctional protein crosslinker with impressive cytocompatibility and biocompatibility (Zhang et al., 2011a). It is commercially available and synthesized by the reaction between a carboxylic acid and *N*-hydroxysuccinimide (NHS) in the presence of carbodiimides. It is known as a derivatizing agent that target primary amine groups (Abello et al., 2007). In the field of peptide synthesis, NHS or 1-hydroxybenzotriazole has been shown to be valuable intermediates because of their high reactivity. The reactive group is used to activate the carboxylic acid of the amino acid residue immobilized on the resin before amide bond formation (Bich et al., 2010).

Since fibroin protein consists of only small fraction of lysine amino acid (Table 2.1). It was suspected that the available sites for a chemically crosslinked reaction with the NHSP along the polypeptide chain may not be high enough to facilitate a stable hydrogel network formation. Thus, the gel enhancer, poly(*L*-lysine) (PLL, chemical structure shown in Figure 2.5), was also be incorporated into the reaction mixture. PLL, a partial synthetic polypeptide is currently available in a wide

range of molecular weights and architectures. It can be degraded by cells effort and has been used as a delivery vehicle for small drugs (Shukla et al., 2012).

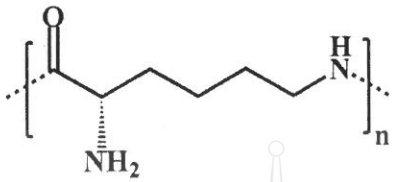

Figure 2.5 Chemical structure of poly(*L*-lysine) (PLL).

Last but not least, the combined use of the two polypeptides may produce a new permanent polyion-complex hydrogel with improved mechanical properties, pronounced water resistance, while maintaining its biocompatibility and biodegradability over a period time. A permanent polyion-complex hydrogel, consisting of a primary chemically-crosslinked network of gelatin physically linked with the pectin by the electrostatic interactions, was successfully prepared and the resultant material showed impressive mechanical properties and water resistance (Farris et al., 2009). For the case of SF-PLL systems, it is likely that both macromolecules can bind to the NHSP, thus forming amide linkages and so, the primary crosslinked network. The electrostatic associations of SF and PLL are likely to occur between the positively charged amine groups of PLL and the negatively charged carboxylic groups of glutamate, aspartate or both acidic moieties (Table 2.1). Several advantages of using PLL as a gelation enhancer, particularly for SF systems, are listed on Table 2.2.

Table 2.2 Advantages of using PLL to promote SF gelation.

Advantages
1. Enhanced chemically crosslinked SF network.
2. Allow the formation of a new "permanent polyion-complex" hydrogel, *in situ*, with improved and tunable mechanical properties and water resistance.
3. Provide the SF hydrogel a *smart* "pH-responsive character", thus making it more suitable for specific biomedical applications.
4. Promote the cell adhesion and proliferation onto the SF hydrogel.

Additionally, PLL are commercially available in three different molecular structures, as shown in Figure 2.6; α-PLL, ε-PLL and α-PDLL (Kokufuta et al., 2011). This availability may allow the fabrication of crosslinked SF/PLL hydrogels with different morphologies and so different properties, thus creating a wide range of novel materials for both tissue engineering and pharmaceutical applications.

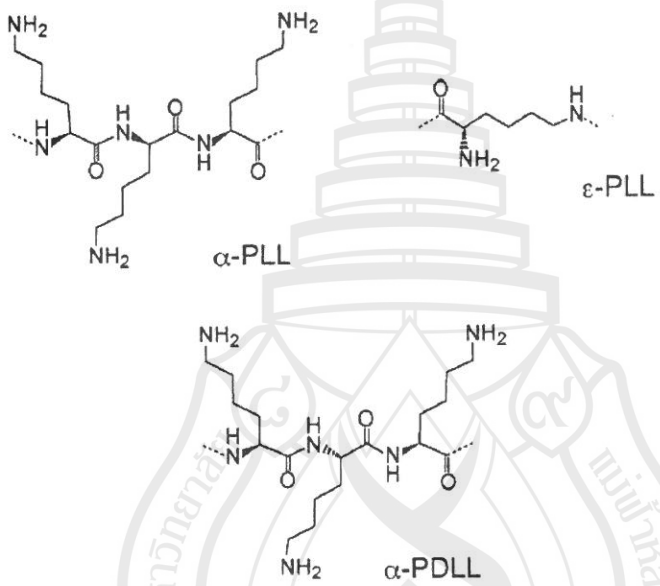

Figure 2.6 Three poly(lysine) samples available for the gel preparation. α-PLL, a homopolymer of *L*-lysine; α-PDLL, a copolymer of *L*-lysine and *D*-lysine (racemic mixture); ε-PLL, a homopolymer consisting of the *L*-lysine residues linked by the peptide bonds between the ε-amino group and the α-carboxyl groups (Kokufuta et al., 2011).

Several parameters, such as the SF/crosslinker mass ratio, reaction time, sonication and physicochemical properties of regenerated SF, may play important roles on crosslinking efficiency of the proposed methods. Furthermore, an understanding of silk gelation and its influencing is necessary for the design and structural engineering the silk-based biomaterials. These features therefore, needed to be evaluated for a development of silk-based biomaterials to suit specific needs for a wider range of applications.

2.5 α-Mangostin

G. mangoatana belongs to the family of Clusiaceae and commonly known as mangosteen. It is cultivated in the tropical rainforest and mainly found in Malaya, India, Thailand, Vietnam, Singapore, Philippines and Burma (Pedraza-Chaverri, 2008, Zadernowski et al., 2009). The mangosteen tree is very slow-growing with a straight stem and a pyramidal crown. It attains 6-25 m in height and has dark-brown or nearly black color bark. The inner bark contains yellow and bitter gummy latex. The leaves are short oval or elliptic, dark-green and slightly glossy (9-25 cm length and 4.5-10 cm width). Flowers are green with red spots on the outside and yellowish-red on the inside. They have around 4-5 cm width and may be male or hermaphrodite on the same tree. A cross-section of a peel is red and around 6-10 mm thick. The fruit is round with diameter of up to 7.5 cm. It appears red-purple from the outside and contains white flesh from the inside (Zadernowski et al., 2009, Morton and Miami, 1987). *G. mangostana* pericarp contains secondary metabolites, such as prenylated and oxygenated xanthones, including the α-, β- and γ-mangostins, garcinone E, 8-deoxygartanin, gartanin, mangostenol, and mangostenone (Pedraza-Chaverri, 2008). Xanthones from mangosteen fruit display various biological properties, such as antioxidant, antitumoral, anti-inflammatory, anti-allergy, antibacterial, antifungal and antiviral activities (Chen et al., 2008a, Yoshikawa et al., 1994, Williams et al., 1995, Mahabusarakam et al., 2000, Pedraza-Chaverri, 2008). For example, α-mangostin isolated from mangosteen fruit pericarp showed highest inhibition of leukemia cell lines HL60, K562, NB4 and U937 (IC_{50} of 5–10 μM). The antitumoral activity of mangostin has been observed in mouse mammary organ culture with an IC_{50} of 1.0 μg/mL (2.44 μM) (Matsumoto et al., 2004). It also displayed cytotoxicity against DLD-1 cells (20 μM). Furthermore, α-mangostin showed antimicrobial activities against *S. aureus* (both normal and penicillin-resistant strains) with MIC values of 1.56–12.5 μg/mL (Mahabusarakam et al., 1986). Therefore, α-mangostin is a promising natural compound for drug discovery and pharmaceutical applications.

CHAPTER 3
EXPERIMENTAL METHODS

3.1 Preparation and Characterization of Silk Fibroin Hydrogels

3.1.1 Chemicals

Bombyx mori silk cocoons were kindly supplied from the Silk Innovation Center (SIC), Mahasarakham University, Thailand. The cocoons were kept in air dried room temperature. Poly(ethylene glycol)diacrylate (PEGDA), *O,O'*-bis[2-(*N*-succinimidyl succinylamino)ethyl]polyethylene glycol (NHSP), calcium chloride ($CaCl_2$) anhydrous and sodium carbonate (Na_2CO_3) were purchased from the Sigma-Aldrich and used without purification. All other chemicals were purchased from the Sigma-Aldrich.

3.1.2 Preparation of Regenerated Silk Fibroin (RSF)

The dried cocoons were boiled twice in an aqueous solution of Na_2CO_3 for 30 min to remove sericin protein. The silk fibroin (SF) was then dissolved in different solvent system, either the mixed solvent of $CaCl_2$/EtOH/H_2O (mole ratio of 1:2:8), or the aqueous solution of a 9.3 M lithium bromide (LiBr) for 3 hr. The fibroin solution was dialyzed in a cellulose dialysis tube (MWCO = 3,500) against deionized water for 3 days. After that, RSF solution was freeze-dried to obtain the protein powder. A protein recovery was calculated using Equation (1).

Protein recovery (%) = (Final mass/ Initial mass) x 100 ---------- (1)

3.1.3 Preparation of Physically Crosslinked Silk Fibroin Hydrogels

The RSF solutions were firstly prepared by dissolving appropriate amount of RSF powder in deionized water (0.7 mL) prior to transferring into a test tube. The solution was then incubated at room temperature for until there is a pronounced increase in the apparent viscosity (resistance to flow). The duration of time to reach to this point is referred, herein, as a "gelation time". To establish the effects of the PEGDA addition, a 0.3 mL of the PEGDA was added into the RSF solutions prior to incubation at room temperature. The gelation times of the RSF in the presence of PEGDA were also evaluated using similar method as described above. The feed compositions of the samples are illustrated in Table 3.1.

3.1.4 Preparation of Chemically Crosslinked Silk Fibroin Hydrogels

For the chemical crosslinking, an aqueous solution of RSF (0.5 ml) and NHSP (0.5 ml) were thoroughly mixed in HEPES buffer at 37 °C to allow a chemical crosslinking reaction to occur. The total solid weight of SF and NHSP was kept constant at 15% (w/v) and the weight ratios of NHSP to SF were varied from 1:1, 1:2 and 1:5. The feed compositions of all hydrogel samples are illustrated in Table 3.1. For the preparation of the freeze-dried samples, the freshly prepared hydrogel was immersed in deionized water (pH 5.6) for 2 days at room temperature. After that, it was frozen in liquid nitrogen, prior to lyophilization at -40°C for 20 h.

Table 3.1 Feed compositions of the SF-based samples.

Sample	Composition (%w/v)			Weight ratio of NHSP/SF	Ultrasonication
	NHSP	SF	PEGDA		
SF2	-	2	-	-	No
SF4	-	4	-	-	No
SF6	-	6	-	-	No
SF8	-	8	-	-	No
SF10	-	10	-	-	No
SF2PEG	-	2	30	-	No
SF4PEG	-	4	30	-	No
SF6PEG	-	6	30	-	No
SF8PEG	-	8	30	-	No
SF10PEG	-	10	30	-	No
SF2PEGU	-	2	30	-	Yes
SF4PEGU	-	4	30	-	Yes
SF6PEGU	-	6	30	-	Yes
SF8PEGU	-	8	30	-	Yes
SF10PEGU	-	10	30	-	Yes
NHSP/SF	7.5	7.5	-	1:1	No
NHSP/2SF	5	10	-	1:2	No
NHSP/5SF	2.5	12.5	-	1:5	No

3.1.5 The Effect of Ultrasonication

To study the effect of ultrasonication on the silk gelation, the feed formulations from Sections 3.1.3 and 3.1.4 were subjected to ultrasonic wave for 40 s prior to incubation at room temperature. After completion of the sol-gel transition, the gelation times were recorded using similar method as described previously.

3.1.6 Characterization

A molecular weight range of the regenerated SF obtained from Section 3.1.2 was determined by using a 10% of polyacrylamide gel. The sample loading was at least 5:1 and the protein concentration was more than 0.02 g/ml.

The sol-gel fraction of the SF gels was determined using Equation (2). Briefly, the gels were dried in an oven for 24 hr. After that, the dried gels were weighed (W_d), followed by swollen in deionized water. Finally, the gels were re-dried in an oven for 24 hr and their weights were measured (W_{rd}).

$$\text{Sol fraction (\%)} = [(W_d - W_{rd}) / W_d] \times 100 \quad \text{---------- (2)}$$

A structural transition of SF was evaluated by using the Fourier Transform Infrared (FTIR) spectroscopy. The freeze-dried samples were mixed with potassium bromide (KBr) powder and their FTIR spectra were obtained using Spectrum GX (Perkin-Elmer) in the spectral region of 400-4,000 cm^{-1} with 32 scans and 4 cm^{-1} resolution.

The morphology of the freeze-dried samples was evaluated by using the Scanning Electron Microscopy (SEM). SEM images were acquired after gold sputtering at accelerated voltage of 15 kV and at 16 mm working distance.

A thermal analysis of the freeze-dried samples was performed by ADSC822E differential scanning calorimeter (Mettler Toledo) and a TGA/SDTA851E thermogravimetric analyzer (Mettler Toledo). The thermograms were obtained using a nitrogen flow rate of 20 mL/min and scanning rate of 10°C/min. For the DSC and TGA, the samples were heated from 25°C to 220°C and from 25°C to 600°C, respectively.

3.2 Chemical Investigation and Antibacterial Activity of α-Mangostin

3.2.1 Raw Materials and Chemicals

The pericarp of *G. mangostana* fruit was chopped and dried. Column chromatography (CC) and quick column chromatography (QCC) were performed on silica gel 100 (0.063-0.200 mm, Merck, Germany) and silica gel 60 (0.063-0.230 mm, Merck, Germany), respectively. Pre-coated thin layer chromatography (TLC) aluminum sheets of silica gel 60 F_{254} (20x20 cm, layer thickness 0.2 mm, Merck,

Germany) were used for analytical purposes and the compounds were visualized under ultraviolet light or anisaldehyde-sulfuric acid and vanillic acid spraying reagents. Organic solvents for extraction and chromatography distilled at their boiling point ranges prior to use. Solvents for UV and IR were analytical grade reagents (BDH HiperSolv^{TM} for HPLC/VWR International Ltd.).

The nutrient agar (CRITERION dehydrated culture media), dimethyl sulfoxide (DMSO) and Tween20 were used for evaluation of antimicrobial activity. Five microorganism cultures (*Escherichia coli* TISTR 780, *Psudomonas aeruginosa* TISTR 781, *Salmonella typhimurium* TISTR 292, *Bacillus cereus* TISTR 687, and *Staphylococcus aureus* TISTR 1466) were derived from the Microbiological Resources Center of the Thailand Institute of Scientific and Technological Research and kept as stock cultures at the Microbiology Laboratory in Mae Fah Luang University. The microorganism methicillin-resistant *Staphylococcus aureus* SK1 was obtained from the Department of Microbiology, Faculty of Science, Prince of Songkla University, Thailand.

3.2.2 Extraction and Isolation of α-mangostin

The dried pericarp of *G. mangostana* (1.93 kg) was immersed in acetone at room temperature (7 L, 6 days). The residue was further immersed in acetone at room temperature (7 L, 6 days). The filtered solution was evaporated to dryness under reduced pressure to yield viscous crude acetone extract (234.50 g).

3.2.3 Purification of α-Mangostin from *G. mangostana*

A portion of the acetone extract of the pericarp fruit of *G. mangostana* (35.0 g) was subjected to quick column chromatography (QCC) using silica gel (Merck 60, 40-63 μm) as the stationary phase packed inside the 60 mm length column (120 g) and eluted (250 ml each) with gradient hexane; hexane-CH_2Cl_2, CH_2Cl_2-Me_2CO and Me_2CO. On the basis of their TLC characteristics, the collected fractions, containing the same major components, were combined to afford twenty fractions (1-20). Fraction 3 (2.83 g) was further purified by column chromatography (CC) with diameter 46 mm, length of 600 mm, and eluted with CH_2Cl_2-hexane (1:1 v/v) to give seven subtractions (3.1-3.7). The subfraction 3.2 (1.40 g), containing α-mangostin as a major component, was finally recrystallized in the mixture of hexane-CH_2Cl_2 (2:3) to

give α-mangostin, 1.0 g. Fraction 4 (1.20 g) was further purified by column chromatography (CC) with diameter 46 mm, length of 600 mm, and eluted with CH_2Cl_2-hexane (1:1 v/v) to give five subtractions (4.1-4.5). The subfractions 4.2 (440.0 mg) and 4.3 (660.0 mg) containing α-mangostin as a major component, were finally recrystallized in the mixture of hexane-CH_2Cl_2 (2:3) to give α-mangostin, 320.0 mg and 540 mg, respectively.

3.2.4 Characterization Techniques

The melting points were measured in degree Celsius (°C) and were uncorrected, using a digital Electrothermal BÜCHI Melting Point B-540 Melting Point Apparatus. Ultraviolet spectra (UV) were recorded using UV-Vis spectrometer (Perkin Elmer Lambda, United States of America). Principle bands (λ_{max}) were recorded as wavelengths (nm) and log ε in methanol solution. Infrared spectra (IR) were recorded on Perkin-Elmer FTSFT IR/Spectrum spectrometer at United States of America. Major bands (ν_{max}) were recorded in wavenumber (cm^{-1}). ^{1}H and ^{13}C nuclear magnetic resonance spectra were recorded on Brüker FTNMR Ultra Shield 400 MHz at Germany. Spectrum were recorded in acetone-d_6 solution and recorded as chemical shift (δ) value in ppm down field from TMS (internal standard δ0.00).

3.2.5 Antibacterial Activity Assay

The six bacteria strains, Gram-positive (*B. cereus*, *S. aureus* and MRSA) and Gram-negative (*E. coli*, *Ps. aeruginosa* and *S. typhimurium*) were chosen for the evaluation of the biological activity of the drug-loaded SF matrices. These microorganisms are the most common pathogenic bacteria that cause infectious diseases, including the tuberculosis, pneumonia, cellulitis and typhoid fever.

3.2.5.1 Determination of Minimum Inhibition Concentrations (MICs)

Minimum inhibition concentrations (MICs) were determined by the broth micro dilution method (CLSI, 2002). Test samples were dissolved in DMSO. Serial 2-fold dilutions of the test samples were mixed with melted MHB in microtiter plates. Final concentration of crude extracts and isolated compound in broth ranged from 1,280-2.5 µg/mL and 128-0.25 µg/mL, respectively. Add 50 µL of inoculum suspensions in each well (final concentration of $1x10^4$ CFU/well). The inoculated plates were incubated at 35-37 °C for 16-18 h, 0.18% resazurin 10 µL was dropped in

microtiter plate and incubated in 35-37 ºC for 2-3 h. The blue color indicated that the sample can inhibit bacterial growth, while the pink color indicated that the samples cannot inhibit bacterial growth. MICs were recorded by reading the lowest concentration that inhibited visible growth. The tests were performed at least in triplicate. Vancomycin and gentamicin were used as positive control drugs.

3.2.5.2 Antibacterial Activity by Agar Disc Diffusion Method

The paper disc diffusion method was used to screen the antibacterial of silk fibroin samples (Lorian, 1996). Three to five colonies of bacterial culture were transferred to nutrient broth and incubated for 3 hr at 37°C, maintaining under shaking condition (150 rpm). The turbidity of bacterial suspension was adjusted by using a 0.85% NaCl (normal saline solution, NSS), comparing to a 0.5 McFarland standard. The cell culture was determined using total plate count. The culture was swabbed onto an agar plate using a sterile cotton swab. Sterile filter paper was placed on the agar plates, containing the microorganism. Then, around 10 and 20 mg of silk fibroin sample were placed on the agar plate. The plates were kept in the incubator at 37°C for 18 hr. The test was performed in triplicate for each sample. A diameter of clear zone shown on plates was then measured in millimeters and was identified as its antimicrobial activity. Antibiotic paper disc for control marker of antibacterial activity was vancomycin and streptomycin. All samples were coded as shown in Table 3.2.

Table 3.2 Description of the test samples.

No.	Sample	Description
1	1GD	1 mg/mL of crude extract in DMSO
2	1GTW	1 mg/mL of crude extract in Tween20/water (0.01:0.99)
3	10GD	10 mg/mL of crude extract in DMSO
4	10GTW	10 mg/mL of crude extract in Tween20/water (0.02:0.98)
5	MD	α-mangostin in DMSO
6	MTW	α-mangostin in Tween20/water (0.01:0.99)
7	MT	α-mangostin in Tween20
8	MDW	α-mangostin in DMSO/water (0.8:0.2)
9	SD	Silk fibroin in DMSO
10	SW	Silk fibroin in water
11	SDS	Silk fibroin in DMSO (shake)
12	SDV	Silk fibroin in DMSO (vortex)
13	SWS	Silk fibroin in water (shake)
14	SWV	Silk fibroin in water (vortex)
15	SSD	Sericin in DMSO
16	SSW	Sericin in water
17	WT	Water/Tween20 (1:1)
18	T20	Poly(oxyethylene sorbitan monolaurate) (Tween20)
19	W	Water
20	PD	PEGDA in DMSO
21	PW	PEGDA in water
22	D	Dimethyl sulfoxide (DMSO)
23	PL	Poly (*L*-lysine)
24	4SFPEGW	Silk fibroin/PEGDA hydrogel (4% fibroin in water)
25	6SFPEGW	Silk fibroin/PEGDA hydrogel (6% fibroin in water)
26	8SFPEGW	Silk fibroin/PEGDA hydrogel (8% fibroin in water)
27	10SFPEGW	Silk fibroin/PEGDA hydrogel (10% fibroin in water)
28	8SFPEGD	Silk fibroin/PEGDA hydrogel (8% fibroin in DMSO)
29	10SFPEGD	Silk fibroin hydrogel (10% fibroin in DMSO)

CHAPTER 4
RESULTS AND DISCUSSIONS

4.1 Preparation and Characterization of Physically Crosslinked Silk Fibroin Hydrogels

4.1.1 Protein Recovery

Silk fibroin (SF) can be separated from the silk sericin (SS) *in vitro* and dissolved in water by using a variety of salt solutions, leading to a transparent solution of regenerated silk fibroin (RSF) (Altman et al., 2003, Hardy et al., 2008). To our best knowledge, the effects of extraction solvent on the protein recovery and its physicochemical properties have not yet been systematically clarified. This study, therefore, performed a comparative study to evaluate these correlations. The freeze-dried RSF sample extracted from and a ternary $CaCl_2$/EtOH/Water (1:2:8 mole ratio) solvent mixture is pale yellow in color (Figure 4.1), similarly to that from an aqueous solution of LiBr. The aqueous RSF samples from the two extraction solvents are also quite similar. They are clear yellow as shown in Figure 4.1.

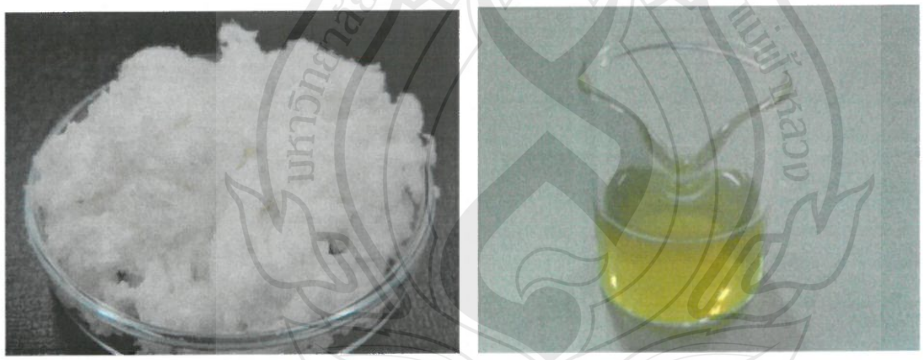

Figure 4.1 Regenerated silk fibroin (RSF) powder extracted from a ternary solvent (left) and its aqueous form (right).

Despite these, the % protein recovery of the sample extracted from a ternary solvent is found to be higher than that from a LiBr solution (see Table 4.1). As compared to a LiBr salt, a $CaCl_2$ is a stronger chaotropic agent which could directly interact with the hydrogen peptide bond in the polypeptide chains thus, making it more soluble (salting-in) in an aqueous media (Hardy et al., 2008, Sah and Pramanik, 2010).

Table 4.1 Percentage of silk fibroin recovery in different solvent systems.

	Solvent system			
	LiBr/Water		$CaCl_2$/EtOH/Water	
	1	2	1	2
Initial mass (g)	1.01	1.01	4.03	4.51
Final mass (g)	0.42	0.32	1.85	2.15
Protein recovery (%)	41.27	31.66	45.78	47.80

4.1.2 Molecular Weight Range

Sodium dodecyl sulfate polyacrylamide gels electrophoresis (SDS-PAGE) is a technique used in biochemistry, genetic and molecular biology to separate protein as well as to roughly estimate the molecular weight of the protein of interest. In this study, the SDS-PAGE was employed to examine the range of molecular weight of RSF by comparing the distance travelled in relative to the standard protein markers (15-170 kDa).

Figure 4.2 SDS-PAGE Electrophoresis of aqueous solutions of RSF extracted from; a ternary solvent mixture (Lane 1-5) and an aqueous solution of lithium bromide (LiBr) (Lane 6-9).

Figure 4.2 shows the electrophoretic patterns of an aqueous solution of RSF (band 1-5) extracted from a ternary solvent. It is found that all RSF samples show a broad dull band from 35-130 kDa, indicating a mixture of the medium chains and the light chains (25-35 kDa) (Um et al., 2001). The medium SF chains may be

obtained from the degradation of the heavy chains (350 kDa) of raw silk protein during degumming and dissolution in a solvent system. The fact that all SF samples display similar electrophoretic pattern confirms a good extraction repeatability of the method used in this project. The protein recovery using this method is found to be within a range of 40-50% (Table 4.1) consistent with the SF content in the silk raw material previously reported (Sah and Pramanik, 2010).

For the case of the RSF obtained from LiBr extraction, there is no electrophoretic pattern appeared between 15-170 kDa (Figure 4.2, Lane 6-9), illustrating a huge impact of the selected extraction solvent on the resultant molecular weight rage in RSF sample. It is worth mentioning that the molecular weight of RSF from LiBr extraction may be either higher than 170 kDa or lower than 15 kDa. Additional experiments thus, need to be performed to clarify this postulation.

4.1.3 Silk Gelation

Gelation time of SF formulations, containing different SF concentrations, was examined by incubation, each formulation, at room temperature for until the macroscopic sol-gel transition was visually observed (e.g., a marked increase in viscosity). This study aimed to lay fundamental groundwork to gain a better understanding of a silk gelation under *in vitro* conditions. Details from this study would be useful for a design of appropriate experimental conditions, employed for a subsequent chemically crosslinking reaction. Table 4.2 presents the gelation time of RSF aqueous solutions extracted from the two solvent systems. It is found that the 4% (w/v) RSF extracted from a ternary solvent turns gel (or another words, undergoes a sol-gel transition) within 13 days, while that from a LiBr solution, there is no sign of gelation over a whole experiment period. For the case of the ternary-extracted sample, the process is found to be accelerated by the increased SF content as evidenced by the decreased gelation time from 13 days of the 4% silk-containing sample to 10 days of the 8% silk-containing sample (Figure 4.3). Furthermore, the addition of the PEGDA is found to promote the gelation kinetics of SF as confirmed by the shortened gelation time of the 4% silk-containing sample from 13 days to 3 days (Table 4.2 and Figure 4.3). The explanation for this may be correlated with the greater extent of physical crosslink density provided along the peptide chains. It is believed that PEGDA alters the hydrophobic hydration sphere of the silk protein by

breaking the hydrogen bonding between the water and the polypeptide. This reduces the water molecules around the polypeptide and then, facilitates them to collide (folding or salting-out) with each other, leading to an accelerated silk gelation (Hardy et al., 2008).

As seen in Figure 4.3, the applied ultrasonication slightly slows down the silk gelation, in contrast with the previous works (Wang et al., 2008). This surprising result could be explained in terms of the possible degradation of SF during sonication. For the subsequent studies, one needs to take this issue into consideration to avoid any undesired reaction. Up until now, it can be said that both a ternary solvent extraction and the addition of PEGDA enhance a α-to-β transition in the silk protein and this eventually accelerates the formation of the silk gel (gelation).

Table 4.2 Visual observation of the gels from RSF extracted by different solvent systems in the presence and absence of PEGDA.

Solvent system	RSF (%w/v)	PEGDA (%w/v)	Gel formation	Gelation time (day)	Visual observation
$CaCl_2/EtOH/H_2O$	4	-	Yes	13	
	4	30	Yes	3	
	8	30	Yes	2	
$LiBr/H_2O$	4	30	No	-	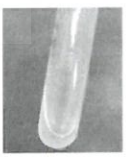
	8	30	No	-	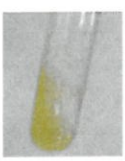

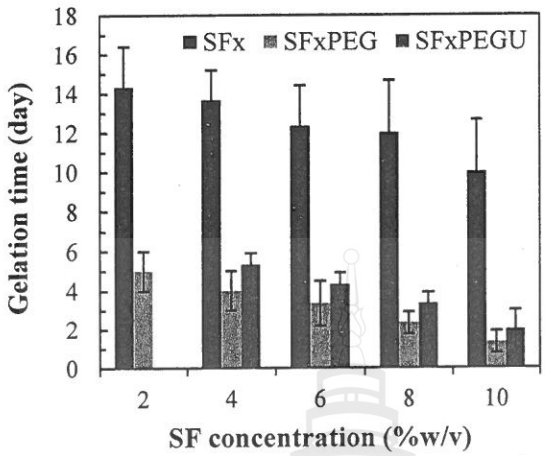

Figure 4.3 Gelation time of difference RSF aqueous formulations in the absence (SFx) and in the presence of PEGDA, with (SFxPEGU) and without (SFxPEG) the use of ultrasonication.

4.1.4 Water Resistance

The water resistance of different SF gels was determined in terms of the sol-gel fraction (%). This parameter indicates the proportion of gel (water-insoluble) fraction remained after dissolution in an aqueous media. The lower the sol fraction, the greater water resistance and so, the more suitable would the material become for biomedical applications. As seen in Figure 4.4, the maximum and the minimum averaged sol-gel fractions of SF gel from the unmodified RSF (4-10% w/v) are around 45% and 17%, respectively. The sol fraction decreases with an increasing of the SF content. This pronounced water resistance perhaps associated with the increased crosslinking density in the SF-enriched formulations to enhance a network formation in the sample. When the SF content is further increased (i.e., 12, 14%), it is believed that the resultant material would display even lower sol-fraction, comparing to the 10% SF sample. However, the material would also be expected to have smaller porous structure that ultimately prohibits the passive diffusion of cells, nutrients or other active compounds. Thus, there might be an optimal range of silk composition for a suitable design of silk-based hydrogel matrices.

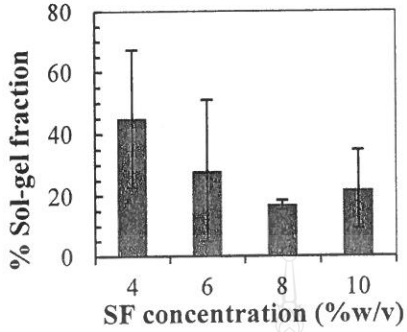

Figure 4.4 Sol-gel fraction of different unmodified SF gels.

The sol-gel fractions (%) of the PEGDA-containing gels (SFPEG) from RSF solutions extracted by a ternary solvent extraction are shown in Figure 4.5. The sol-fractions of all gels are varied between 80-85%, depending on the silk concentration. The higher the silk concentration, the lower the sol-fraction and so the more stable would the gel become.

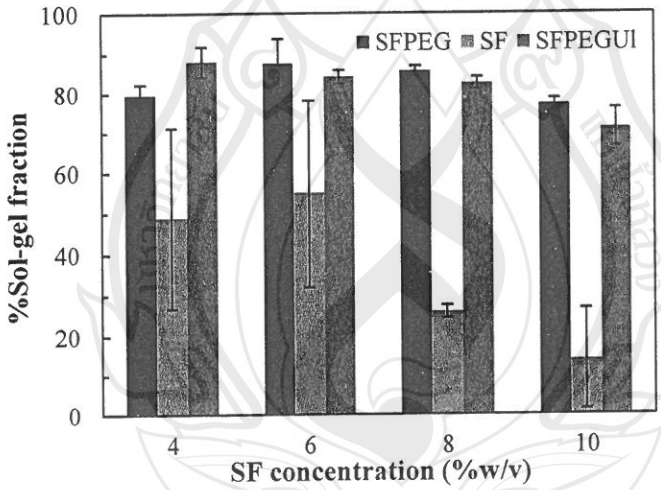

Figure 4.5 Sol-gel fraction of unmodified SF gels (SF) and accelerated SF gels with (SFPEGU) and without (SFPEG) the uses of ultrasonication.

Interesting results may be obtained when comparing the unmodified SF with the PEGDA-containing samples. It is found that the sol fraction of unmodified SF gels is generally lower than that of the PEGDA-containing samples, meaning that the unmodified gels are stronger with greater water stability. The sol-gel transition of an aqueous RSF has been reported as an irreversible process primarily driven by β-sheet crystallization (Matsumoto et al., 2006, Nagarkar et al., 2010). The gelation kinetics show typical characteristic of a nucleation and growth process which are

noticed by a relatively long induction period, followed by a rapid gelation. In the induction period, the protein molecules spontaneously self-aggregate by the intra- and intermolecular hydrophobic associations to form the physical crosslinks that eventually transform into a mature irreversible β-sheet stacking structure. A whole process occurs over long time scales. Once the protein has completely turned into the crystalline β-pleated structure, the resultant material possesses maximum water stability and mechanical properties. For the case of the PEGDA addition, the polyalcohol competitively interacts with water molecules, thus promoting the hydrophobic associations of the protein in the initial period. As a result, the polypeptide would have tighter physically crosslinked network, explaining the accelerated gelation kinetics. Since this gelation is promoted by the addition of the inducer (PEGDA) and not in local thermodynamic equilibrium, one would expect the PEGDA-containing system to maintain higher sol (water-soluble) fraction with some extents of crystalline imperfection. Additionally, the data points of all unmodified SF gels show wider standard deviations as compared to those of the PEGDA-induced SF gels (Figure 4.4 and Figure 4.5). This finding confirms that the unmodified SF gelation is neither controllable, nor reproducible, thus highlighting a high impact of using PEGDA to improve gelation kinetics, water resistance and processability. The association behavior of silk fibroin is rather complicated and that, it could be affected by a number of parameters. For examples, the experimental conditions used for degumming and extracting of SF, as well as the purification method employed are of important as it determines a range of molecular weight, protein recovery, source of impurity and aging stability of aqueous RSF. The presence of calcium salt in RSF was believed to primarily take part on the varied silk gelation kinetics. When the content of this contaminant is increased, the silk hydrogelation may occur within shorter period of time. Similar behavior was also published (Wang and Zhang, 2013). Additionally, it may be possible that SF may undergo thermal decomposition during degumming and extraction processes at above 80°C, resulting in the decreased chain segments and the lesser extent of the molecular chain packing into the β-sheet structure. Ones thus, need to take all these into consideration to minimize the sources of errors and obtain the material with reliable properties for professional usages.

4.1.5 Structural Analysis

FTIR spectra of freeze-dried RSF samples obtained from the two extraction solvents and their data analysis are shown in Figure 4.6 and Table 4.3, respectively. It is worth mentioning that typical FTIR spectra of SF show vibrational bands between 1630-1660 cm^{-1}, 1520-1540 cm^{-1} and 1230-1270 cm^{-1}, corresponding to the amide I (C=O stretching), amide II (N-H bonding), and amide III (C-N stretching), respectively (Matsumoto et al., 2006, Kweon et al., 2001, Mandal et al., 2009b). As seen in Table 4.3, RSF obtained by LiBr extraction (RSFL) shows characteristic peaks at 1656 cm^{-1} (amide I), 1545 cm^{-1} (amide II) and 1245 cm^{-1} (amide III), all attributed to the α-helical (random coil) structure. For the case of RSF extracted by a ternary solvent (RSFC), these peaks are slightly shifted toward lower wavenumber region, illustrating the potential co-existence of the β-sheet together with a random coil structure (Chen et al., 2001, Matsumoto et al., 2006). It is possible that during dissolution of the fibroin, ethanol, as part of a ternary solvent, can partially induce a structural transition of the protein into the β-sheet structure.

Table 4.3 FTIR analysis of RSF samples extracted by different solvent systems.

Formulation	-OH	C=O stretching	Amide I (C=O stretching)	Amide II (C-N stretching)	Amide III (C-N stretching)
RSFC	3298	-	1654	1541	1246
RSFL	3287	-	1656	1545	1245
SF10	3286	-	1625	1532	1247
SF10PEG	3283	1723	1624	1517	1252

FTIR data analysis of unmodified SF gel (SF10) and the PEGDA-containing SF gel (SF10PEG) are also shown in Table 4.3. Interestingly, both SF10 and SF10PEG gels display a characteristic band at around 1625 cm^{-1}, attributed to the vibrational amide I in fibroin. This band is shifted towards lower region as compared to that of the RSFC sample (1654 cm^{-1}), suggesting a preferential transformation of SF from a random coil to a pleated structure. Moreover, a shift of the amide II band from 1541 cm^{-1} (RSFC) to around 1532 cm^{-1} for the SF10, and to around 1517 cm^{-1} for the SF10PEG, also confirmed this α-to-β (sol-to-gel) phase transition during

gelation. For SF10PEG, there is a new absorption band at around 1723 cm^{-1}, corresponding to an asymmetric stretching of the C=O group in PEGDA. The fact that the amide II signal of SF10PEG appears at 1517 cm^{-1}, even lower than that found in SF10, re-confirms a high impact of PEGDA to induce a phase transformation in SF as discussed earlier.

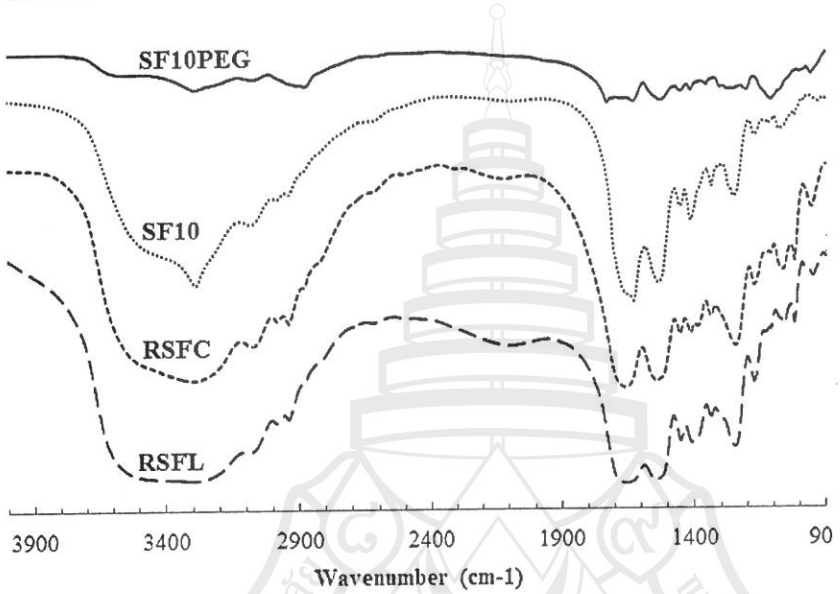

Figure 4.6 FTIR spectra of SF10PEG, SF10, RSFC and RSFL. All spectra were recorded from 400-4000 cm^{-1}.

4.1.6 Morphological Studies

SEM micrographs of unmodified SF4, SF8 and SF10 gels (ternary solvent extraction) are present in Figure 4.7. The SF4 and SF8 gels possess a porous structure with typical characteristic of open interconnected network and brittle material (Figure 4.7a-b). For SF10, the gel still shows characteristic of brittle material but with a well-defined interconnected porous structure (Figure 4.7c). Such architecture stabilizes the gel and explains the improved physicochemical properties and gelation kinetics of the sample previously mentioned. As seen in Figure 4.7d-f, all PEGDA-containing gels (SF4PEG, SF8PEG and SF10PEG) exhibit denser interconnected porous structure with thicker wall boundary, as compared to the unmodified gels of the same fibroin contents. As the silk fibroin content is increased, the gel shows a coexistence of typical random organization (amorphous) together with a lamellar structure (crystalline). This finding also re-assures the PEGDA-induced structural transformation to speed up the silk hydrogelation process.

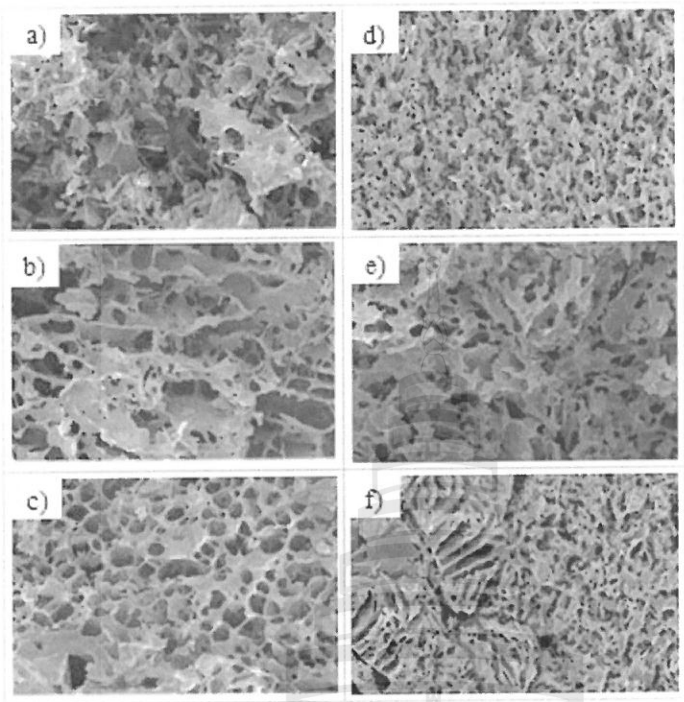

Figure 4.7 SEM micrographs of; (a) 4SF, (b) 8SF, (c) 10SF, (d) SF4PEG, (e) SF8PEG and (f) SF10PEG. All gels were obtained from a ternary-extracted RSF solution and the images were taken at magnification of 500x.

4.1.7 Thermal Analysis

Thermogravimetric analysis (TGA) was employed to investigate the chemical changes of the samples as well as to proof the existence of newly-formed intermolecular interactions through their increased thermal stability. The 1st derivative of TG plots of RSF samples, extracted from a ternary solvent (RSFC) and a LiBr solution (RSFL), are shown in Figure 4.8 and Table 4.4. As may be observed, the RSFC and RSFL display two degradation patterns with around 45% mass remaining. The first stage between 50-100°C is perhaps responsible for the evaporation of semi-bound water in RSF samples. The second stage between 250-550°C may be correlated to the decomposition of side chain groups of proteins such as glycine and alanine.

Table 4.4 Thermal properties of the freeze-dried RSF samples and the SF gel.

Sample	$T_{d,max}$ (°C)	
	1	2
RSFL	81.4	298.8
RSFC	80.6	314.2
SF10	91.8	311.0
SF10PEG	103.0	344.8

As expected, RSFC sample displays higher $T_{d,max}$ (314°C), as compared to RSFL (299°C). The result implies greater β-sheet content in the former, highlighting a stronger effect of a ternary solvent to promote the α-to-β phase transformation during extraction and hydrogelation processes of SF. This is supported by the shifts of amide I and amide II absorption bands towards even lower wavenumber for the case of RSFC as described in the FTIR results (Figure 4.6). For the SF10PEG, the gel displays the $T_{d,max}$ value at around 345 °C, significantly higher than those of RSFL and RSFC (Table 4.4). The increased thermal stability is primarily associated with the stronger intermolecular interactions induced by the PEGDA and so, the tighter crosslinking network formed in the hydrogel.

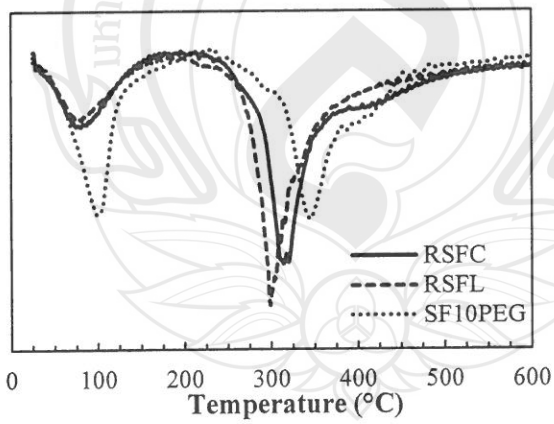

Figure 4.8 The 1st derivative of TG plots of the freeze-dried RSF samples extracted by a ternary solvent (RSFC) and an aqueous LiBr (RSFL). A 1st derivative plot of SF10 and SF10PEG were also shown for comparison.

4.2 Preparation and Characterization of Chemically Crosslinked Silk Fibroin Hydrogels

4.2.1 Crosslinking Reaction

The chemically crosslinked hydrogels were prepared by acylation reaction of SF and NHSP. The reaction mechanism is shown in Figure 4.9 (Wong and Jameson, 2011, Bich et al., 2010). Since NHSP is a homobifunctional amine-specific protein crosslinker, it would theoretically react on the primary amine groups ($-NH_2$) of the silk protein to form amide bonds and eliminate *N*-hydroxysuccinimide as the leaving group (Bich et al., 2010). In order to facilitate additional binding sites with NHSP, poly (*L*-lysine) (PLL), at a final concentration of 0.01% (w/v), was introduced into a system as the gel enhancer. This, as an optional, was aimed to enhance a stable hydrogel network formation. Once a crosslinking has taken place, the viscosity of a RSF solution steadily increases, until reaching a point of flow resistance (Figure 4.10). At this point, SF has undergone a sol-gel transition (or another words, gelation) to form a stable 3D-hydrogel network within 24 hr. The resultant network strengthens and improves mechanical stability of the hydrogels in an aqueous media (water resistance) as seen in Figure 4.10.

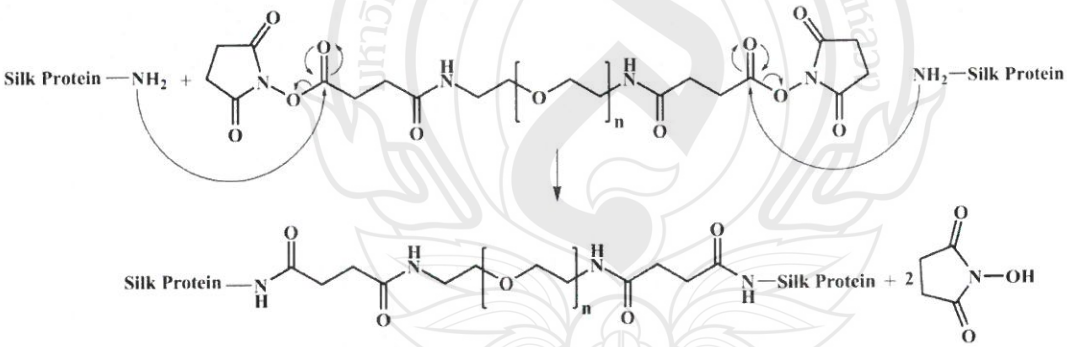

Figure 4.9 The reaction machanism of SF and NHSP through acylation reaction.

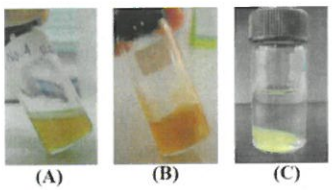

Figure 4.10 The transition of SF from the sol (A) to the gel (B) state by acylation reaction of NHSP, resulting in the improved water resistance of the material in an aqueous media (C).

4.2.2 Water Resistance

The most important property of hydrogels is the ability to absorp large amount of water, while maintaing their structural integrity. The gel fraction of the hydrogels implies the degree of crosslinking within the materials. The higher the gel fraction, the higher degree of crosslinking and thus, the more water resistance would the materials become. As seen in Table 4.5, the NHSP/SF hydrogel shows the percentage of gel fraction of around 54%, implying that the hydrogel lose around 46% of its mass during extraction process. The loss or sol fraction may be due to the unreacted compounds or low-mlecular weight peptide components.

Table 4.5 Gel fraction (%) of the unmodified and NHSP/SF hydrogels.

Sample	Gel fraction (%)
NHSP/SF	54.36±5.20
NHSP/2SF	68.03±3.64
NHSP/5SF	76.74±1.51
SF10	74.24±0.95

As the weight ratio of SF/NHSP is increased, the resultant hydrogels (NHSP/2SF and NHSP/5SF) display increased gel fraction (%). This indicateds that the high SF content systems may be more favorable for the crosslinking reaction and so, a formation of stable hydrogel network. Since the *B. mori* SF has relatively low contents of both lysine (0.4 mol%) and arginine (0.5 mol%) amino acid (Sashina et al., 2006), the crosslinking sites should be low in number and kinetics. Therefore, a high fibroin content is required to achieve highly efficient inter-chain crosslinking reaction and to produce the mechanically stable network hydrogels.

4.2.3 Structural Analysis

FTIR spectroscopy was used to prove the sol-gel (or α-to-β) transition during crosslinking and the incorporation of NHSP in the silk-based matrices. The spectra of RSFC powder, unmodified and all crosslinked SF hydrogels are presented in Figure 4.11. Their data analysis was also summarized in Table 4.6. Typical FTIR spectrum of SF shows vibrational bands between 1630-1660 cm^{-1}, 1520-1540 cm^{-1} and 1230-1270 cm^{-1}, corresponding to the amide I (C=O stretching), amide II (N-H bonding), and amide III (C-N stretching), respectively (Matsumoto et al., 2006, Chen

et al., 2001). For the freeze-dried RSFC, the spectrum shows characteristic peaks at 1658 cm^{-1} (amide I), 1541 cm^{-1} (amide II) and 1241 cm^{-1} (amide III), suggesting its preferential existence in an α-helical (random coil) structure. For the unmodified SF10 and all crosslinked hydrogels (NHSP/5SF, NHSP/5SF/PLL), the vibrational bands at amide I, II and III are shifted towards lower region. This implies a transformation of SF from α-helix to β-sheet structure (Chen et al., 2001). As expected, the spectra of NHSP/5SF and NHSP/5SF/PLL hydrogels in Figure 4.11 exhibit the characteristic peak of the ether linkage (C-O-C) of NHSP molecule, at around 1102 cm^{-1} (Moonsri et al., 2008). This confirms the incorporation of NHSP within SF matrices.

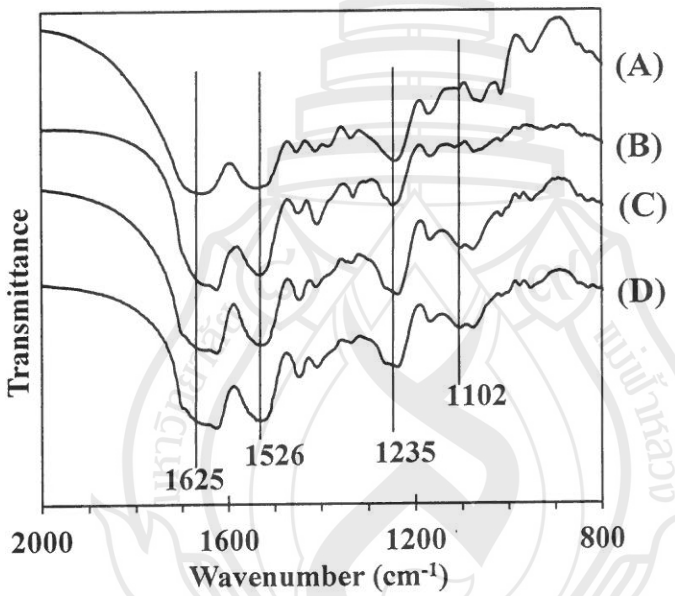

Figure 4.11 FTIR spectra of; RSFC powder (A), unmodified SF hydrogel (B), crosslinked NHSP/5SF hydrogel (C) and crosslinked NHSP/5SF/PLL hydrogel (D). Spectra were recorded from 800-2000 cm^{-1}.

Table 4.6 FTIR data analysis of RSF powder, unmodified and chemically crosslinked SF hydrogels.

Sample	Amide I (cm^{-1})	Amide II (cm^{-1})	Amide III (cm^{-1})	Ether (C-O-C) (cm^{-1})
RSFC	1658	1541	1241	-
SF10	1625	1532	1247	-
NHSP/5SF	1625	1529	1236	1102
NHSP/5SF/PLL	1626	1527	1235	1102

4.2.4 Morphological Studies

SEM micrographs of all hydrogels are present in Figure 4.12. It is found that unmodified SF10 hydrogel (or pure sample) showed irregular porous structure with typical characteristic of a honey comb-like and brittle porous structure (Figure 4.12A). For the PLL-containing crosslinked hydrogel (NHSP/5SF/PLL), the material exhibits a well-defined three-dimensional (3D) architecture of interconnected porosity with high content of β-pleated structure (Figure 4.12B). This ordered arrangement of the protein appears to be more uniform in the PLL-free crosslinked sample (NHSP/5SF in Figure 4.12C). A few notes can be made from this point. First, PLL is really an optional for the formation of a stable hydrogel network. Without the addition of PLL, a more stable and homogeneous hydrogel network is apparently observed (Figure 4.12C). It then leads to a second point that is, PLL strongly interacts with SF molecules and interferes the molecular packing of the protein. By changing the PLL feed composition, one would expect to obtain crosslinked SF-based hydrogels with controllable pore architectures.

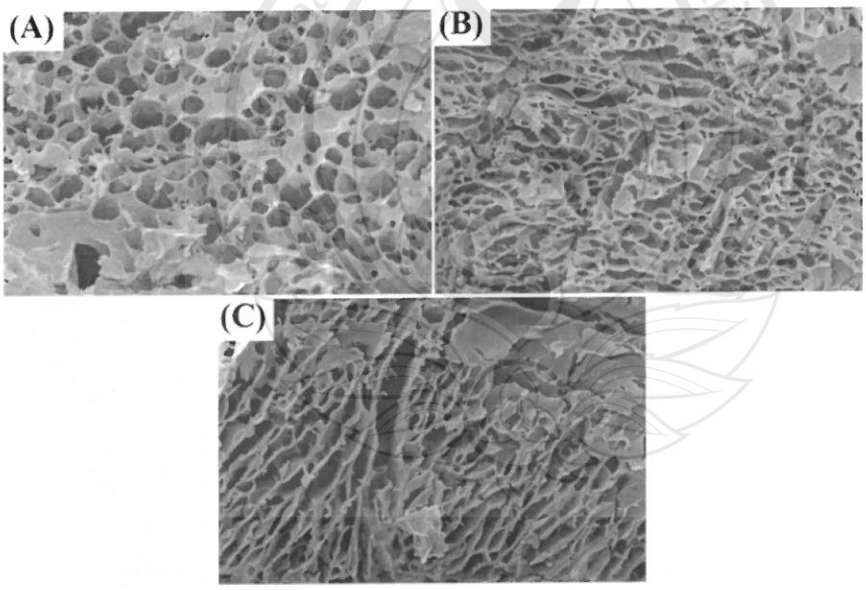

Figure 4.12 SEM micrographs of; unmodified SF10 (A), crosslinked NHSP/5SF/PLL (B) and NHSP/5SF (C). Images were taken at magnification of 500x. Arrows indicate the formation of a stable β-pleated structure.

4.3 Chemical Investigation and Antibacterial Activity of α-Mangostin

4.3.1 Chemical Investigation

The major chemical constituent of acetone-extracted *G. mangostana* from the pericarp of mangosteen fruit is proven to be α-mangostin. The structure of the compound is elucidated by the spectroscopic 2D-NMR techniques. The spectral data has been compared with those previously reported in the literature (Ee et al., 2006).

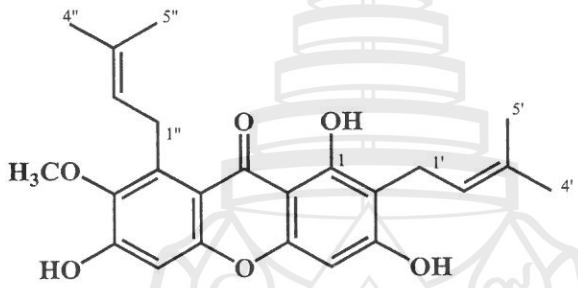

The isolated α-mangostin appears as a yellow solid with a melting point of 182-183°C, similarly to those reported in the literatures (Yates and George, 1958, Ahmad et al., 2012). The UV spectrum of the isolate in methanol shows the maximum absorption bands (log ε) at 243.2 (4.53), 259.8 (4.40), 316.3 (4.43) and 357.98 (3.90) (Figure 4.13). It shows the major IR absorption bands, corresponding to the conjugated carbonyl group at 1641 cm^{-1}, hydroxyl group at 3360 cm^{-1}, aromatic ring at 1570 cm^{-1} and the methoxy group at 2913 cm^{-1} (Figure 4.14). The ^{1}H NMR spectrum, presented in Figure 4.15 and Table 4.7, reveals the presence of four sharp *singlet* signals at δ 13.75 (1-OH), 6.76 (H-5), 6.34 (H-4) and 3.78 (7-OCH_3). The signals of the two prenyl side chains are also observed. Those signals are the two *broad triplet* signals of the two olefinic protons (δ 5.26 (2H)), two *doublet* signals of the benzylic methylene protons (δ 4.08 and 3.32) and three *singlet* signals of the four methyl groups (δ 1.81, 1.73, and 1.64 (6H)). The ^{13}C NMR spectrum, as shown in Table 4.7 and Figure 4.16, display twenty-four carbons and quaternary signal at δ 182.6, attributing to the carbonyl carbon of ketone form. The location of the prenyl units at C-2 and C-8 is supported by the HMBC correlations of H-1′ to C-1, C-2, C-2',

C-3', C-5' and H-1″ to C-7, C-8, C-8a, C-2", C-3", C-5", respectively (Table 4.7 and Figure 4.17). The position of the 3-OH and 6-OH is deduced by the resonances of an oxygen-bearing carbons at δ 162.7 (C-3) and 157.0 (C-6), respectively. The methoxy proton at δ 3.78 shows potent correlation with those at δ 144.2, indicating that it has been attached at C-7. The isolated compound is then identified as α-mangostin (Ee et al., 2006).

Table 4.7 The NMR spectral data of α-mangostin.

Position	δ_H (multiplicity, J_{Hz})	δc	HMBC
1	13.75 (1H, *s*)	161.5	C-1, C-2, C-9, C-9a
2	-	110.8	-
3	-	162.7	-
4	6.34 (1H, *s*)	92.9	C-2, C-3, C-4a, C-9, C-9a
4a		155.4	-
5	6.76 (1H, *s*)	102.5	C-6, C-8a, C-9, C-10a
6	-	157.0	-
7	-	144.2	-
8	-	137.8	-
8a	-	111.8	-
9	-	182.6	-
9a	-	103.4	-
10a	-	155.9	-
1'	3.32 (2H, *d*, J = 7.2 Hz)	21.8	C-1, C-2, C-2', C-3', C-5'
2'	5.26 (1H, *t*, J = 7.2 Hz)	124.7	C-1', C-4'
3'	-	131.1	-
4'	1.81 (3H, *s*)	18.1	C-2', C-3', C-5'
5'	1.64 (3H, *s*)	25.7	C-2', C-3', C-4'
1"	4.08 (2H, *d*, J = 7.2 Hz)	26.6	C-7, C-8, C-8a, C-2", C-3", C-5"
2"	5.26 (1H, *t*, J = 7.2 Hz)	123.4	C-1", C-4"
3"	-	131.1	-
4"	1.64 (3H, *s*)	25.7	C-2", C-3", C-5"
5"	1.73 (3H, *s*)	17.2	C-2", C-3", C-4"
7-OCH_3	3.78 (3H, *s*)	61.1	C-7

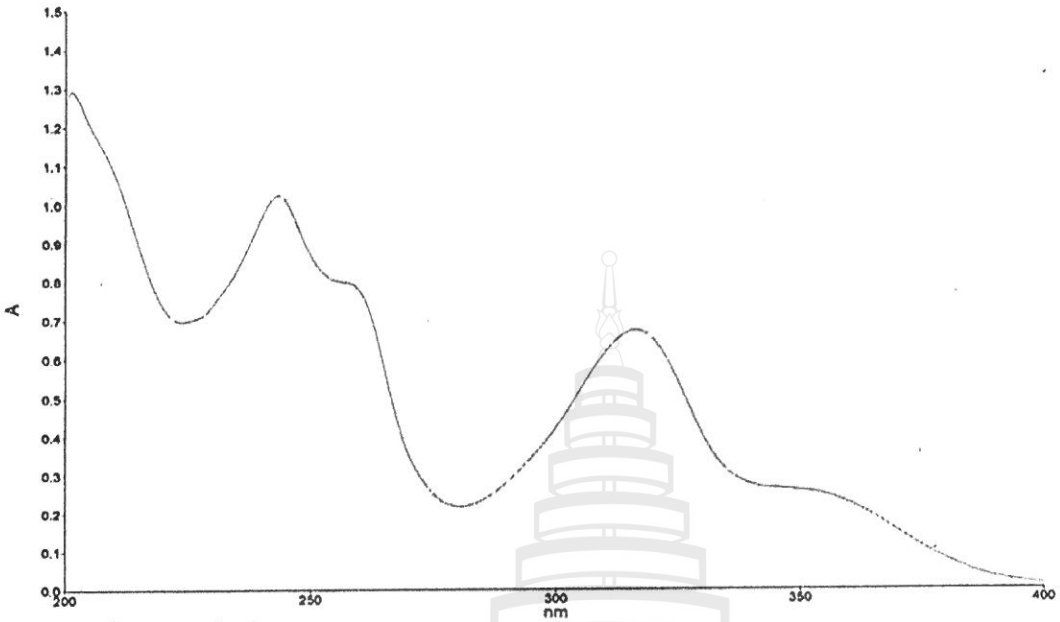

Figure 4.13 UV spectrum of α-mangostin.

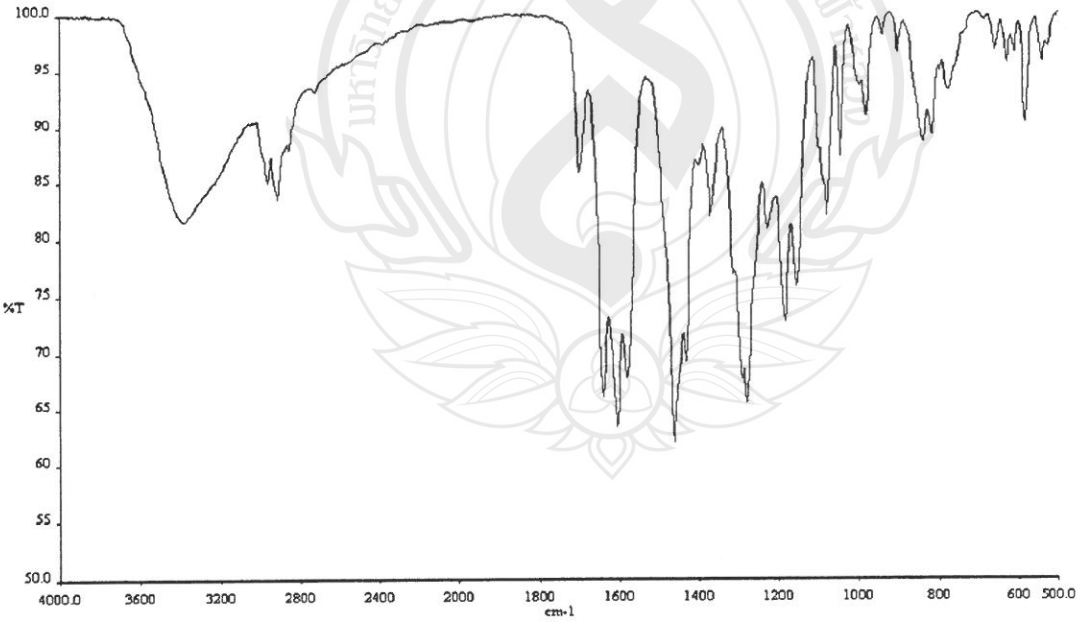

Figure 4.14 IR spectrum of α-mangostin.

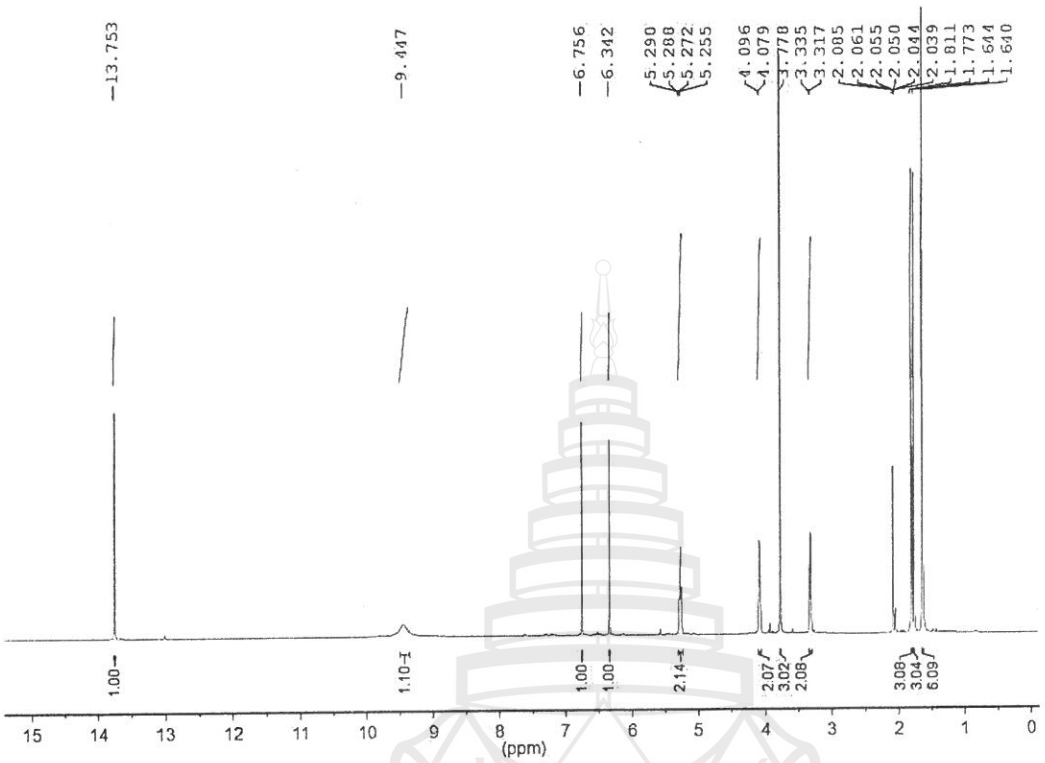

Figure 4.15 ^{1}H NMR (400 MHz) (Acetone-d_6) spectrum of α-mangostin.

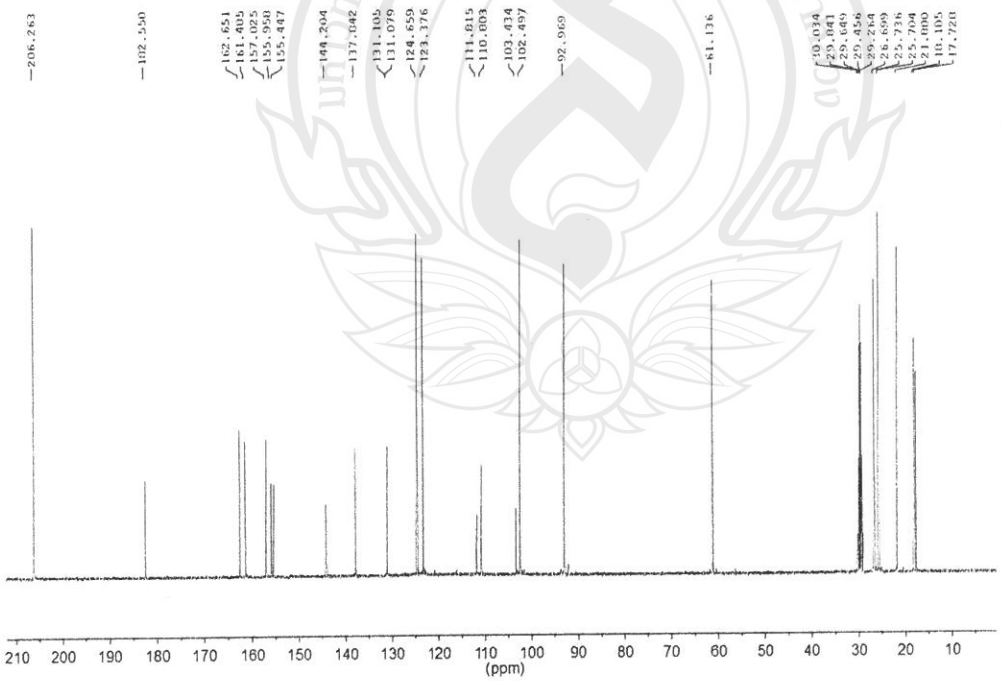

Figure 4.16 ^{13}C NMR (100 MHz) (Acetone-d_6) spectrum of α-mangostin.

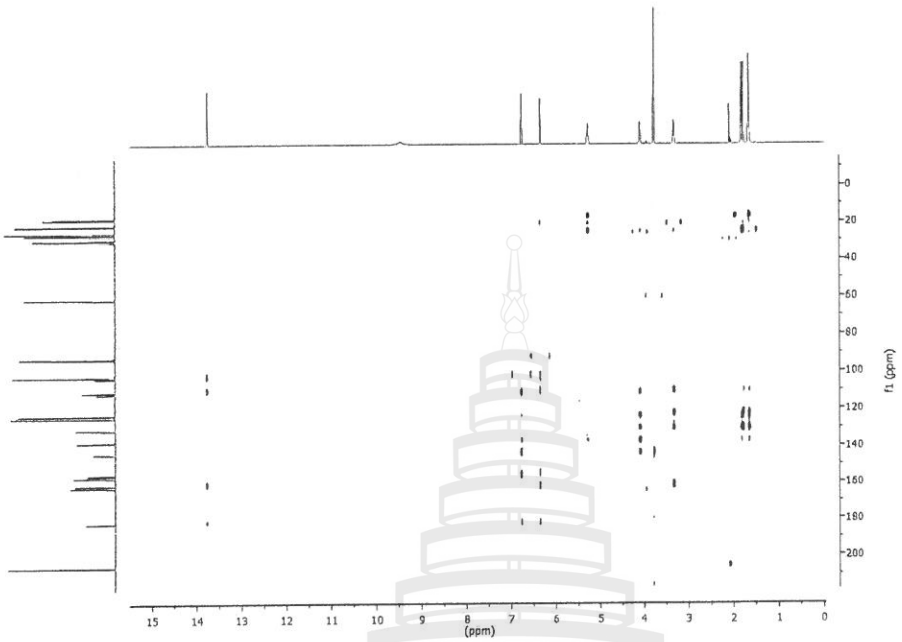

Figure 4.17 HMBC spectrum of α-mangostin.

4.3.2 Evaluation of Antibacterial Assay

4.3.2.1 Broth Microdilution Method

As seen in Table 4.8, the 1GD and 10GD of *G. mangostana* crude extracts dissolved in DMSO exhibit strong antibacterial activity against Gram-positive *B. cereus,* MRSA-SK1 and *S. aureus* with the MICs ranges of 4.0-8.0 and 2.5-5.0 µg/mL, respectively. Whereas, these extracts in water (1GW and 10GW) exhibit inactive against Gram-positive bacteria (entries 1-4). α-Mangostin in DMSO (MD) shows excellent antibacterial activity with MIC value of 0.25 µg/mL (entry 5), against Gram-positive bacteria, comparing to the standard drugs. A nonionic emulsifying agent, Tween 20, was chosen to mix with water to render the solubility of α-mangostin in an aqueous media. It is found that α-mangostin in a mixed water/Tween20 (MTW) show inactive antibacterial activity. However, the active compound in a mixture of DMSO and water (DMSO/water = 0.8:0.2) shows moderate antibacterial activity against Gram-positive with MICs range of 32-64 µg/mL (entries 6-8). Overall work finding indicates that the biological activity of α-mangostin depends on its solubility in a given dissolution media. The silk fibroin and sericin

(entries 9-12), dissolved in DMSO and DMSO/water (SD, SSD, SW, SSW) show inactive antibacterial activity. Likewise, the controlled Tween20, sterilized water and Tween20/water samples exhibit inactive antibacterial activity (entries 13-15; T20, W, TW). These results imply that the regenerated silk fibroin and sericin solutions should have little or no antibacterial activity.

Interestingly, α-mangostin shows selective inhibition of Gram-positive *E.coli*, *Ps. aeruginosa* and *S. typhimurium*, but not against Gram-negative bacteria. This could be explained in terms of morphological differences among these microorganisms. It is known that Gram-negative pathogens are composed of an outer phospholipidic membrane with structural lipopolysaccharide components (Jaiganesh and Arunachalam, 2011). This makes the cell wall impermeable to lipophilic solutes. Their porins constitute also acts as a selective barrier to hydrophilic solutes with an exclusion limit of about 600 Da (Jaiganesh and Arunachalam, 2011). In another hand, the Gram-positive bacteria are composed of the less effective peptido glycone layers (Jaiganesh and Arunachalam, 2011). This feature makes them more susceptible to solutes, as compared to the Gram-negative ones. From another point of view, *G. mangostana* extract and α-mangostin exhibit antibacterial activity because of its typical phenolic toxicity to microorganism. The reason why α-mangostin in DMSO (MD) shows greater antibacterial activity than *G. mangostana*, extracted in DMSO (1GD and 10GD), is perhaps associated with its pure phenolic compound.

Table 4.8 MICs values of test sample.

No.	Sample	MICs (μg/mL)					
		Gram-positive bacteria			Gram-negative bacteria		
		B. cereus	MRSA-SK1	*S. aureus*	*E. coli*	*Ps. aeruginosa*	*S. typhimurium*
1	1GD	4.0	4.0	8.0	128	128	128
2	1GTW	>128	>128	>128	>128	>128	>128
3	10GD	2.5	5.0	2.5	1280	1280	1280
4	10GTW	>1280	>1280	>1280	>1280	>1280	>1280
5	MD	0.25	0.25	0.25	128	128	128
6	MTW	>128	>128	>128	>128	>128	>128

Table 4.8 MICs values of test sample (continued).

No.	Sample	MICs (μg/mL)					
		Gram-positive bacteria			Gram-negative bacteria		
		B. cereus	MRSA-SK1	*S. aureus*	*E. coli*	*Ps. aeruginosa*	*S. typhimurium*
7	MT	0.5	>128	>128	>128	128	>128
8	MDW	32	64	64	>128	>128	>128
9	SD	1280	>1280	>1280	1280	1280	1280
10	SW	>1280	>1280	>1280	>1280	>1280	>1280
11	SSD	1280	1280	>1280	1280	1280	1280
12	SSW	>1280	>1280	>1280	>1280	>1280	>1280
13	WT	>1280	>1280	>1280	>1280	>1280	>1280
14	T20	>1280	>1280	>1280	>1280	>1280	>1280
15	W	>1280	>1280	>1280	>1280	>1280	>1280
Vancomycin (standard drugs)		2.0	1.0	0.5	-	-	-
Gentamicin		-	-	-	2.0	2.0	1.0

4.3.2.2 Agar Disc Diffusion Method

Antibacterial activity of SF hydrogels was evaluated by Agar disc diffusion method against 6 strains of microorganisms. The antibacterial activity of silk fibroin hydrogels, containing different percentages by weight of SF to PEGDA (10%, 15%, 20% and 25%) in water was shown in Table 4.9. It is found that the PEGDA-containing silk hydrogels show weak to moderate antibacterial activity against Gram-positive *B. cereus,* MRSA-SK1 and *S. aureus,* as evidenced by the diameters of the inhibition zone between 9.2 ± 1.2 - 10.9 ± 10.6, 5.7 ± 1.2 - 6.1 ± 0.6 and 5.7 ± 1.1 - 6.2 ± 0.6 mm, respectively. In addition, all silk fibroin hydrogel samples show inactive antibacterial activity against Gram-negative bacteria (*E. coli*, *Ps. aeruginosa* and *S. typhimurium*). When DMSO was used as a dissolution media, the PEGDA-containing silk hydrogels (SF8PEGD and SF10PEGD) displayed larger inhibition zone, comparing to those in water (Table 4.9). For example, the inhibition

zones against *B. cereus*, MRSA-SK1 and *S. aureus* increase to 14.1 ± 0.6 mm, 6.9 ± 0.6 mm and 6.9 ± 1.2 mm, respectively. It is worth noting that the increased antibacterial activity of the PEG-containing hydrogels may arise from the activity of PEGDA on its own. This is evidenced by the inhibition zones of PEGDA against Gram-positive bacteria (*B. cereus,* MRSA-SK1 and *S. aureus*), as shown in Table 4.10. However, there may be synergetic effects of PEGDA and SF to enhance antibacterial activity, as indicated by an increasing of inhibition diameter against *B. cereus* from 8.4 ± 0.6 mm (PD, Table 4.10) to 14.1 ± 0.6 mm (SF10PEGD, Table 4.9). Additional experiments need to be conducted to clarify this ambiguity.

Table 4.9 Diameter of clear zone (mm) for different silk hydrogel samples.

Code	SF (% w/w)	PEGDA (% w/w)	Weight of sample	Diameter of clear zone (mm) ± S.D					
				Gram-positive			Gram-negative		
				B. cereus	MRSA-SK1	*S. aureus*	*E. coli*	*Ps. aeruginosa*	*S. typhimurium*
SF4PEGW	10%	90%	10 mg	9.2 ± 1.2	5.7 ± 1.2	5.7 ± 1.1	inactive	inactive	inactive
			20 mg	9.2 ± 0.6	5.8 ± 0.6	5.7 ± 0.6	inactive	inactive	inactive
SF6PEGW	15%	85%	10 mg	9.3 ± 0.6	5.9 ± 1.1	5.9 ± 1.1	inactive	inactive	inactive
			20 mg	9.9 ± 0.6	5.9 ± 0.6	5.9 ± 0.6	inactive	inactive	inactive
SF8PEGW	20%	80%	10 mg	9.9 ± 1.1	5.9 ± 1.1	5.9 ± 1.1	inactive	inactive	inactive
			20 mg	9.9 ± 1.1	5.8 ± 1.1	5.8 ± 1.1	inactive	inactive	inactive
SF10PEGW	25%	75%	10 mg	9.2 ± 1.2	6.0 ± 1.2	6.1 ± 0.6	inactive	inactive	inactive
			20 mg	10.9 ± 0.6	6.1 ± 0.6	6.2 ± 0.6	inactive	inactive	inactive
SF8PEGD	20%	80%	10 mg	13.1 ± 0.6	6.4 ± 0.5	6.4 ± 0.5	inactive	inactive	inactive
SF10PEGD	25%	75%	10 mg	14.1 ± 0.6	6.9 ± 0.6	6.9 ± 0.6	inactive	inactive	inactive
Vancomycin				17.1 ± 0.6	20.6 ± 1.1	19.0 ± 0.8	inactive	inactive	inactive
Streptomycin				-	-	-	21.6 ± 1.1	20.0 ± 0.9	19.6 ± 1.1

Table 4.10 Diameter of clear zone (mm) for different chemicals used in this study.

Code	Diameter of clear zone (mm) ± S.D					
	Gram-positive			Gram-negative		
	B. cereus	MRSA-SK1	*S. aureus*	*E. coli*	*Ps. aeruginosa*	*S. typhimurium*
SD	5.9 ± 1.1	inactive	inactive	5.8 ± 0.6	5.9 ± 1.1	5.8 ± 1.1
SW	Inactive	inactive	inactive	inactive	inactive	inactive
PD	8.4 ± 0.6	8.1 ± 0.6	9.0 ± 0.4	inactive	inactive	inactive
PW	8.8 ± 0.6	8.9 ± 0.6	12.4 ± 0.6	inactive	inactive	inactive
W	Inactive	inactive	inactive	inactive	inactive	inactive
D	Inactive	inactive	inactive	inactive	inactive	inactive
PL	Inactive	inactive	8.7 ± 0.6	inactive	inactive	inactive
Vancomycin	17.1 ± 0.6	20.6 ± 1.1	19.0 ± 0.8	inactive	inactive	inactive
Streptomycin	-	-	-	21.6 ± 1.1	20.0 ± 0.9	19.6 ± 1.1

CHAPTER 5
CONCLUSION AND SUGGESTION FOR FURTHER WORK

Over the past decades, naturally-derived hydrogels from the *Bombyx mori* silk fibroin (SF) has increasingly gained interest in both biomedical and pharmaceutical fields due to its excellent properties such as good mechanical properties, ease of fabrication, controllable crystallinity, biodegradability, biocompatibility and non-cytotoxicity. These remarkable properties are related to its structural transition from the α–helix into the β-sheet structure. The transition, occasionally known as a sol-gel transition, is mainly driven by the hydrophobic interactions and the hydrogen bond formation between the polymer chains. The process would eventually lead to the formation of a thermodynamically stable SF hydrogel. Our study demonstrated that various parameters, such as the increased silk concentration, type of extraction solvent, the addition of the inducer and the extent of chemically crosslinking, accelerate the silk gelation kinetics and at the same time, improve physicochemical properties of the fibroin hydrogels. These were proven by the decreased sol-gel fraction (or another words, increased water-resistance), increased mechanical stability and a uniform dense interconnected porous structure. The following are some tips for the preparation of stable SF-based hydrogels with short gelation kinetics (< 24 hr) suited for therapeutic drug delivery applications.

- After degumming process, the remained fibroin residue should be re-extracted in a ternary $CaCl_2$/EtOH/Water solvent system to achieve regenerated silk fibroin (RSF) raw material with appropriate molecular weight range (35-130 kDa) and enhanced protein recovery (45-55% w/w).
- A combined use of SF (4-8% w/v) and the addition of PEGDA (30% w/v) is suggested for the preparation of physically crosslinked hydrogels with tunable gelation time and water resistance.
- For the preparation of chemically crosslinked hydrogels, the optimized SF/NHSP ratio to achieve the most stable, densed and homogeneous network is 1:5. With the addition of PLL, the hydrogels showed a double hydrogel network with larger pore size. This feature offers tunable permeability, biodegradability

and swelling ability to the materials and thus, broadens their practical use as immobilization matrices for cells or drugs.

Both crude and purified forms of the α-mangostin from *G. mangostana* displayed strong antibacterial activity particularly, against the three Gram-positive bacteria; *E. coli, Ps. aeruginosa and S. typhimurium*. Surprisingly, the hydrogel matrices of SF/PEGDA exhibited moderate antibacterial activity against Gram-positive bacteria, including *B. cereus*, *MRSA-SK1* and *S. aureus*. This finding highlights another unexploited property of the hybrid for tissue engineering and biomedical applications.

At this stage, we had gained a better understanding of the *in vitro* SF hydrogelation and could appropriately engineering design of crosslinked SF hydrogel materials. As such, the crosslinked SF hydrogels with satisfied water-swell ability, interior morphology and gelation kinetics were successfully fabricated. In order to evaluate their potential use as a delivery matrix, the release character of the α-mangostin from the materials will need to be performed in the near future. This together with all work finding would allow ones to draw a final conclusion on feasibility of a proposed method to stabilize and improve performance of SF-based hydrogels for therapeutic applications.

REFERENCES

Abdella, P. M., Smith, P. K. & Royer, G. P. 1979. A new cleavable reagent for cross-linking and reversible immobilization of proteins. *Biochem. Biophys. Res. Comm.*, **87,** 734-742.

Abello, N., Postma, H. A. & Bischoff, D. S. 2007. Selective Acrylation of Primary Amines in Peptides and Proteins. *J. Proteome Res.*, **6,** 49-62.

Acharya, C., Hinz, B. & Kundu, S. C. 2008. The effect of lactose-conjugated silk biomaterials on the development of fibrogenic fibroblasts. *Biomaterials,* **29,** 4665-4675.

Ahmad, M., Yamin, B.-M. & Lazim, A.-M. 2012. Preliminary study on dispersion of α-mangostin in PNIPAM microgel system. *Malaysian J. Anal. Sci.*, **16,** 256-261.

Altman, G. H., Diaz, F., Jakuba, C., Calabro, T., Horan, R. L., Chen, J., Lu, H., Richmond, J. & Kaplan, D. L. 2003. Silk-based biomaterials. *Biomaterials*, **24,** 401-416.

Bayraktar, O., Malay, O., Ozgarip, Y. & Batigün, A. 2005. Silk fibroin as a novel coating material for controlled release of theophylline. *Eur. J. Pharm. Biopharm.*, **60,** 373-381.

Bich, C., Maedler, S., Chiesa, K., Degiacomo, F., Bogliotti, N. & Zenobi, R. 2010. Reactivity and applications of new amine reactive cross-linkers for mass spectrometric detection of protein-protein complexes. *Anal. Chem.*, **82,** 172-179.

Chairungsrilerd, N., Takeuchi, K., Ohizumi, Y., Nozoe, S. & Ohta, T. 1996. Mangostanol, a prenyl xanthone from *Garcinia mangostana*. *Phytochemistry,* **43,** 1099-1102.

Chen, F., Porter, D. & Vollrath, F. 2012. Silk cocoon (*Bombyx mori*): Multi-layer structure and mechanical properties. *Acta Biomaterialia,* **8,** 2620-2627.

Chen, L.-G., Yang, L.-L. & Wang, C.-C. 2008a. Anti-inflammatory activity of mangostins from *Garcinia mangostana*. *Food Chem. Toxicol.*, **46,** 688-693.

Chen, P., Kim, H. S., Park, C.-Y., Kim, H.-S., Chin, I.-J. & Jin, H.-J. 2008b. pH-Triggered transition of silk fibroin from spherical micelless to nanofibrils in water. *Macromol. Res.*, **16,** 539-543.

Chen, X., Knight, D. P., Shao, Z. & Vollrath, F. 2001. Regenerated *Bombyx mori* silk solutions studied with rheometry and FTIR. *Polymer,* **42,** 9969-9974.

CLSI 2002. Clinical and Laboratory Standards Institute. Reference method for dilution antimicrobial susceptibility test for bacteria that grow aerobically. Wayne, PA, USA.

Crompton, K. E., Goud, J. D., Bellamkonda, R. V., Gengenbach, T. R., Finkelstein, D. I., Horne, M. K. & Forsythe, J. S. 2007. Polylysine-functionalised thermoresponsive chitosan hydrogel for neural tissue engineering. *Biomaterials,* **28,** 441-449.

Dhandayuthapani, B., Yoshida, Y., Maekawa, T. & Kumar, D. S. 2011. Polymeric scaffolds in tissue engineering application: A Review. *Int. J. Polym. Sci.*, **2011**, 1-19.

Ee, G.C., Daud, S., Taufiq-Yap, Y. H., Ismail, N. H. & Rahmani, M. 2006. Xanthones from *Garcinia mangostana* (Guttiferae). *Nat. Prod. Res.*, **20**, 1067-1073.

Farris, S., Schaich, K. M., Liu, L., Piergiovanni, L. & Yam, K. L. 2009. Development of polyion-complex hydrogels as an alternative approach for the production of bio-based polymers for food packaging applications: A review. *Trends Food Sci. Tech.*, **20**, 316-332.

Garcia-Fuentes, M., Giger, E., Meinel, L. & Merkle, H. P. 2008. The effect of hyaluronic acid on silk fibroin conformation. *Biomaterials*, **29**, 633-642.

Gomes, S., Leonor, I. B., Mano, J. F., Reis, R. L. & Kaplan, D. L. 2012. Natural and genetically engineered proteins for tissue engineering. *Prog. Polym. Sci.*, **1**, 1-17.

Gopalakrishnan, C., Shankaranarayanan, D., Kameswaran, L. & Nazimudeen, S. K. 1980. Effect of mangostin, a xanthone from *Garcinia mangostana* Linn. in immunopathological & inflammatory reactions. *Indian J. Exp. Biol.*, **18**, 843-846.

Hardy, J. G., Römer, L. M. & Scheibel, T. R. 2008. Polymeric materials based on silk proteins. *Polymer*, **49**, 4309-4327.

Hennink, W. & Nostrum, C. V. 2002. Novel crosslinking methods to design hydrogels. *Adv. Drug Deliv. Rev.*, **54**, 13-36.

Hoffman, A. S. 2002. Hydrogels for biomedical applications. *Adv. Drug Deliv. Rev.*, **54**, 3-12.

Jaiganesh, K. P. & Arunachalam, G. 2011. Preliminary phytochemical screening and antimicrobial potential of *Pterospermum canescens* roxb, (sterculiaceae). *Int. J. Pharm. Pham. Sci.* , **3**, 139-141.

Jin, H.-J., Park, J., Karaeorgiou, V., Kim, U.-J., Valluzzi, R., Cebe, P. & Kaplan, D. L. 2005. Water-stable silk films with reduced β-sheet content. *Adv. Func. Mater.*, **15**, 1241-1247.

Jung, H.-A., Su, B.-N., Keller, W. J., Mehta, R. G. & Kinghorn, A. D. 2006. Antioxidant xanthones from the pericarp of *Garcinia mangostana* (mangosteen). *J. Agric. Food Chem.*, **54**, 2077-2082.

Kang, G. D., Lee, K. H., Ki, C. S. & Park, Y. H. 2004. Crosslinking reaction of phenolic side chains in silk fibroin by tyrosinase. *Fibers and Polymers*, **5**, 234-238.

Ko, D. Y., Shinde, U. P., Yeon, B. & Jeong, B. 2013. Recent progress of *in situ* formed gels for biomedical applications. *Prog. Polym. Sci.*, **38**, 672-701.

Kokufuta, M. K., Sato, S. & Kokufuta, E. 2011. Swelling-shrinking behavior of chemically cross-linked polypeptide gels from poly(α-*l*-lysine), poly(α-*dl*-lysine), poly(ε-*l*-lysine) and thermally prepared poly(lysine): Effects of pH, temperature and additives in the solution. **87**, 299-309.

Kweon, H. Y., Park, S. H., Yeo, J. H., Lee, Y. W. & Cho, C. S. 2001. Preparation of semi-interpenetrating polymer networks composed of silk fibroin and poly(ethylene glycol) macromer. *J. Appl. Polym. Sci.,* **80,** 1848-1853.

Li, M., Lu, S., Wu, Z., Tan, K., Minoura, N. & Kuga, S. 2002. Structure and properties of silk fibroin-poly(vinyl alcohol) gel. *Int. J. Biol. Macromol.,* **30,** 89-94.

Lorian, V. 1996. *Antibiotics in laboratory medicines*. Baltimore, William and Wilkins.

Mahabusarakam, W., Proudfoot, J., Taylor, W. & Croft, K. 2000. Inhibition of lipoprotein oxidation by prenylated xanthones derived from mangosteen. *Free Radic. Res.,* **33,** 643-659.

Mahabusarakam, W., Wiriyachitra, P. & Phongpaichit, S. 1986. Antimicrobial activities of chemical constituents from *G. mangostana* Linn. *J. Sci. Soc. Thailand,* **12,** 239-242.

Mandal, B. B., Kapoor, S. & Kundu, S. C. 2009a. Silk fibroin/polyacrylamide semi-interpenetrating network hydrogels for controlled drug release. *Biomaterials,* **30,** 2826-2836.

Mandal, B. B., Priya, A. S. & Kundu, S. C. 2009b. Novel silk sericin/gelatin 3-D scaffolds and 2-D films: Fabrication and characterization for potential tissue engineering applications. *Acta Biomaterialia,* **5,** 3007-3020.

Matsumoto, A., Chen, J., Collette, A. L., Kim, U.-J., Altman, G. H., Cebe, P. & Kaplan, D. L. 2006. Mechanisms of silk fibroin sol-gel transitions. *J. Phys. Chem. B,* **110,** 21630-21638.

Matsumoto, K., Akao, Y., Yi, H., Ohguchi, K., Ito, T., Tanaka, T., Kobayashi, E., Iinuma, M. & Nozawa, Y. 2004. Preferential target is mitochondria in α-mangostin induced apoptosis in human leukemia HL60 cells. *Bioorg. Med. Chem.,* **22,** 5799-5806.

Mondal, M., Trivedy, K. & Kumar, S. N. 2007. The silk proteins, sericin and fibroin in silkworm, *Bombyx mori* Linn., A review. *Caspian J. Environ. Sci.,* **5,** 63-76.

Moonsri, P., Watanesk, R., Watanesk, S., Niamsup, H. & Deming, R. L. 2008. Fibroin membrane preparation and stabilization by polyethylene glycol diglycidyl ether. *J. Appl. Polym. Sci.,* **108,** 1402-1406.

Morton, J. F. 1987. Mangosteen: *garcinia mangostana L.* In: *Fruits of warm climates*. Miami, FL.

Motta, A., Migliaresi, C., Faccioni, F., Torricelli, P., Fini, M. & Giardino, R. 2004. Fibroin hydrogels for biomedical applications: prepartion, characterization and in vitro cell culture studies. *J. Biomater. Sci. Polym. Edn.,* **15,** 851-864.

Nagarkar, S., Nicolai, T., Chassenieus, C. & Lele, A. 2010. Structure and gelation mechanism of silk hydrogels. *Phys. Chem. Chem. Phys.,* **12,** 3834-3844.

Nakagawa, Y., Iinuma, M., Naoe, T., Nozawa, Y. & Akao, Y. 2007. Characterized mechanism of α-mangostin-induced cell death: caspase-independent apoptosis

with release of endonuclease-G from mitochondria and increased miR-143 expression in human colorectal cancer DLD-1 cells. *Bioorg. Med. Chem.*, **15,** 5620-5628.

Nogueira, G. M., Moraes, M. A., Rodas, A. C. D., Higa, O. Z. & Beppu, M. M. 2011. Hydrogels from silk fibroin metastable solution: Formation and characterization from a biomaterial perspective. *Materials Science and Engineering: C,* **31,** 997-1001.

Numata, K. & Kaplan, D. L. 2010. Silk-based delivery systems of bioactive molecules. *Adv. Drug Deliv. Rev.*, **62,** 1497-1508.

Pedraza-Chaverri, J., Cárdenas-Rodríguez, N., Orozco-Ibarra, M. & Pérez-Rojas, J.M. 2008. Medicinal properties of mangosteen (*Garcinia mangostana*). *Food Chem. Toxicol,* **46,** 3227-3239.

Qiu, B., Stefanos, S., Ma, J., Lalloo, A., Perry, B. A., Leibowitz, M. J., Sinko, P. J. & Stein, S. 2003. A hydrogel prepared by *in situ* cross-linking of a thiol-containing poly(ethylene glycol)-based copolymer: A new biomaterial for protein drug delivery. *Biomaterials* **24,** 11-18.

Rouse, J. G. & Kyke, M. E. V. 2010. A review of keratin-based biomaterials for biomedical applications. *Materials,* **3,** 999-1014.

Sah, M. K. & Pramanik, K. 2010. Regenerated silk fibroin from *B. mori* silk cocoon for tissue engineering applications. *Int. J. Environ. Sci. Dev.*, **1,** 404-408.

Sah, M. K. & Pramanik, K. 2011. Preparation, characterization and *in vitro* study of biocompatible fibroin hydrogel. *Afr. J. Biotechnol.*, **10,** 7878-7892.

Sashina, E. S., Bochek, A. M., Novoselov, N. P. & Kirichenko, D. A. 2006. Structure and solubility of natural silk fibroin. *Russian J. Appl. Chem.*, **79,** 869-876.

Shukla, S. C., Singh, A., Pandey, A. K. & Mishra, A. 2012. Review on production and medical applications of ε-polylysine. *Biochem. Eng. J.*, **65,** 70-81.

Sundaram, B. M., Gopalakrishnan, C., Subramanian, S., Shankaranarayanan, D. & Kameswaran, L. 1983. Antimicrobial activities of *Garcinia mangostana*. *Planta. Med.*, **48,** 59-60.

Tan, H. & Marra, K. G. 2010. Injectable biodegradable hydrogels for tissue engineering applications. *Materials,* **3,** 1746-1767.

Teng, D.-Y., Wu, Z.-M., Zhang, X.-G., Wang, Y.-X., Zheng, C., Wang, Z., Li, C.-X. & Zheng, Z. 2010. Synthesis and characterization of *in situ* cross-linked hydrogel based on self-assembly of thiol-modified chitosan with PEG diacrylate using Michael type addition. *Polymer,* **51,** 639-646.

Um, I. C., Kweon, H. Y., Park, Y. H. & Hudson, S. 2001. Structural characteristics and properties of the regenerated silk fibroin prepared from formic acid. *Int. J. Biol. Macromol.*, **29,** 91-97.

Wang, H.-Y. & Zhang, Y.-Q. 2013. Effect of regeneration of liquid silk fibroin on its structure and characterization. *Soft Matter,* **9,** 138-145.

Wang, X., Kluge, J. A., Leisk, G. G. & Kaplan, D. L. 2008. Sonication-induced gelation of silk fibroin for cell encapsulation. *Biomaterials,* **29,** 1054-1064.

Williams, P., Ongsakul, M., Proudfoot, J., Croft, K. & Beilin, L. 1995. Mangostin inhibits the oxidative modifcation of human low density lipoprotein. *Free Radic. Res.,* **23,** 175-184.

Wong, S. S. & Jameson, D. M. 2011. *Chemistry of protein and nucleic acid cross-linking and conjugation*, CRC Press.

Xiong, S.-Y., Cheng, Y.-D., Liu, Y., Yan, S.-Q., Zhang, Q. & Li, M.-Z. 2011. Effect of polyalcohol on the gelation time and gel structure of silk fibroin. *J. Biomed. Mater. Res. B,* **3,** 236-243.

Yates, P. & George, H.-S. 1958. The structure of Mangostin 1. *J. Am. Chem. Soc.,* **80,** 1691-1700.

Yoshikawa, M., Harada, E., Miki, A., Tsukamoto, K., Qian, L. S., Yamahara, J. & Murakami, N. 1994. Antioxidant constituents from the fruit hulls of mangosteen (*Garcinia mangostana* L.) originating in Vietnam. *Yakugaku Zasshi*, **114**, 129-133.

Zadernowsk, R., Czaplicki, S. & Naczk, M. 2009. Phenolic acid profiles of mangosteen fruits (*Garcinia mangostana*). *Food Chem.,* **112,** 685-689.

Zhang, M., Wu, K. & Li, G. 2011a. Interactions of collagen molecules in the presence of *N*-hydroxysuccinimide activated adipic acid (NHS-AA) as crosslinking agent. *Int. J. Biol. Macromol.,* **49,** 847-854.

Zhang, S., Li, F. & Yu, J. Y. 2011b. Novel cellulose/SPI blend bio-fibers prepared via direct dissolving approach. *J. Eng. Fiber Fabr.,* **6,** 31-37.

Curriculum Vitae

1. General Data

Name: Dr. Patchara Punyamoonwongsa

Contact Address: School of Science, Mae Fah Luang University
333 Moo 1, Tambon Ta-sud, Amphur Muang,
Chiangrai 57100, Thailand

Phone (Office): +66-(0)53-916778

E-mail: patchara@mfu.ac.th

2. Education

Period	Degree	Institution	Year of Graduation
1995-1998	B.Sc. (Chemistry), 2nd-Class Honors	Chiang Mai University, Thailand	1998
1999-2001	M.Sc. (Chemistry)	Chiang Mai University, Thailand	2001
2003- 2008	Ph.D. (Polymer Science)	Aston University, England	2008
2010	Postdoctoral	University of New South Wales	2010

3. Awards and Grant Support

1999-2001: Scholarship Recipient of the National Science and Technology Development Agency (NSTDA) at Chiang Mai University, Chiang Mai, Thailand.

2003-2008: Scholarship Recipient of the Royal Thai Government at Aston University, Birmingham, England.

2010: Endeavour Cheung Kong Research Fellowship of the Australian Government at the University of New South Wales (UNSW), Sydney, Australia.

2009: Research funding of Mae Fah Luang University on the project "Association Behavior of the Synthetic Protein-Lipid Complex Analogues".

2011: Research funding of Mae Fah Luang University on the project "Preparation of the Biodegradable Cellulose Derivative and Silk Fibroin Blend Films".

2013-2014: Research funding of the National Research Council of Thailand (NRCT) on the project "Crosslinked Silk Fibroin Hydrogels for Controlled Release of Natural *alpha*-Mangostin".

4. Work and Academic Experiences

From March 2002 – Present: Lecturer at the School of Science, Mae Fah Luang University, Chiangrai, Thailand.

April – October 2010: Post-doctoral Fellow at the University of New South Wales, Sydney, Australia.

Reviewer: The "Chiang Mai International Conference on Biomaterials & Applications 2011", Chiang Mai, Thailand, 9 - 10 August, 2011.

Reviewer: The "First ASEAN Plus Three Graduate Research Congress (AGRC)", Chiang Mai, Thailand, 1 - 2 March, 2012.

Reviewer: The "Congress on Science and Technology of Thailand (STT38)", Chiang Mai, Thailand, 17 - 19 October, 2012.

Program Committee and Reviewer: The "1st Mae Fah Luang University International Conference 2012 (MFUIC2012)", Chiangrai, Thailand, 29 November - 1 December, 2012.

Reviewer: The "Pure and Applied Chemistry International Conference 2013 (PACCON2013)", Chon Buri, Thailand, 23 - 25 January, 2013.

Chair Person and Reviewer: The "IUPAC World Polymer Congress (MACRO 2014)", Chiang Mai, Thailand, 6-11 July, 2014.

5. Publications and Proceedings

Kamonchanok Thananukul, Pakkamon Jarruwale, Nuchada Suttenun, Pall Thordason and **Patchara Punyamoonwongsa**. A Novel Silk Semi-interpenetrating Network Hydrogel as Potential Biomedical Wound Dressing. *Macromolecular Symposia* (*In Press*).

Patchara Punyamoonwongsa and Nuchada Suttenun. A new Crosslinker for the Preparation of Silk Fibroin Hydrogels. *Macromolecular Symposia* (*In Press*).

Kamonchanok Thananukul, Juraiporn Porkaew, **Patchara Punyamoonwongsa**, Robert Molloy and Brian J. Tighe. Kinetic Studies of the Photopolymerisation of Acrylamide in Aqueous Solution: Effects of Bromoform Addition. *Chiang Mai Journal of Science*. 41(2014) 1-9.

C. Witthayaprapakorn, K. Thananukul, N. Suttenun, **P. Punyamoonwongsa** and Robert Molloy. Preparation of Biodegradable Polymer Blended of Poly(*L*-lactic acid)/Cellulose acetate films in the Solvent Mixture. *Advanced Material Research*. 664(2013), 702-706.

Patchara Punyamoonwongsa, Kamonchanok Thananukul, Parawut Kesornsunt, Winita Punyodom. Plasticized Blends of Cellulose Acetate Butyrate and Poly(butylene succinate) as Biodegradable Plastics. *Burapha Science Journal*. 18;2(2013), 113-123.

P. Punyamoonwongsa and B. Tighe. Association Behavior of the Synthetic Protein-lipid Complex Analogues. *Chiang Mai Journal of Science*. 506(2012), 134-137.

P. Punyamoonwongsa and B. Tighe. A Smart Hydrogel-Based System for Controlled Drug Release. *Chiang Mai Journal of Science*. 32(2005), 471-478.

Patchara Punyamoonwongsa and Nuchada Suttenun. A Novel Method for the Preparation of Silk Fibroin Hydrogel Matrices. Proceeding of the "Pure and Applied Chemistry International Conference (PACCON2014)", Khonkaen, Thailand, January 8-10, 2014.

Patchara Punyamoonwongsa and Nuchada Suttenun. Accelerated Silk Fibroin Gelation by the Addition of the Poly(ethylene glycol)diacrylate. Proceeding of the "39th Congress on Science and Technology of Thailand (STT39)", Bangkok, Thailand, October 21-23, 2013.

Patchara Punyamoonwongsa and Nuchada Suttenun. Synergetic Effects of Solvent System and the Addition of Polyetyleneglycol on the Silk Gelation. Proceeding of the "38th Congress on Science and Technology of Thailand (STT38)", Chiang Mai, Thailand, October 17-19, 2012.

P. Punyamoonwongsa and B. Tighe. Therapeutic Applications of Contact Lenses: pH-Responsive Hydrophobically Associating Micellar Structure for Ophthalmic Delivery of Pirenzepine. Proceedings of the "31st Conference of the British Contact Lens Association", Manchester, UK, May 31-June 3, 2007. Appeared in *Ophthalmic Res.* 2007; 39: (S1). ISSN 0030-3747.

P. Punyamoonwongsa and B. Tighe. Therapeutic Applications of Contact Lenses: pH-Responsive Hydrophobically Associating Micellar Structure for Ophthalmic Delivery of Pirenzepine. Proceedings of the "31st Conference of the British Contact Lens Association", Manchester, UK, May 31-June 3, 2007. Appeared in *Ophthalmic Res.* 2007; 39: (S1). ISSN 0030-3747.

P. Punyamoonwongsa and B. Tighe. Therapeutic Application of Contact Lenses: Myopia and Allergic Eye Disease. Proceedings of the "29th Conference of the British Contact Lens Association", Brighton, UK, June 3-5, 2005. Appeared in *Ophthalmic Res.* 2005; 37: (S1):31. ISSN 0030-3747.

P. Punyamoonwongsa and B.Tighe. Therapeutic Applications of Contact Lenses in Myopia Control. Proceedings of "28th Conference of the British Contact Lens Association", Birmingham, UK, May 24-27, 2004. Appeared in *Ophthalmic Res.* 2004; 36: (S1):83. ISSN 0030-3747.

P. Punyamoonwongsa and B.Tighe. Therapeutic Applications of Contact Lenses in Myopia Control (**prize winner poster**). Proceedings of "Annual European Eye and Vision Research Meeting", Vilamoura, Portugal, September 24-27, 2004. Appeared in *Contact Lens and Anterior Eye*. 2004; 27:125.